

**IMMOBILIZING DNazymes ON SURFACES FOR BIOSENSING  
APPLICATIONS**

**IMMOBILIZING DNazymes ON SURFACES FOR BIOSENSING  
APPLICATIONS**

By

Sahar Esmaeili Samani, B. Eng.

A Thesis

Submitted to the School of Graduate Studies

in Partial Fulfilment of the Requirements

for the Degree

Master of Applied Science

McMaster University

© Copyright by Sahar Esmaeili Samani, March 2019

McMaster University Master of Applied Science (2019) Hamilton,  
Ontario (Chemical Engineering)

TITLE: Immobilizing DNAzymes on surfaces for biosensing applications

AUTHOR: Sahar Esmacili Samani, B. Eng. (Sharif University of Technology, Tehran, Iran)

SUPERVISORS: Dr. Carlos D.M. Filipe  
Dr. Yingfu Li

NUMBER OF PAGES: xvii, 78

## **Abstract**

Pathogenic bacteria pose serious threats to public health and safety. They can cause illness, death, and substantial economic losses. The most widely used bacterial detection methods include cell culturing, antibody-based assays, and nucleic acid amplification techniques, such as polymerase chain reaction (PCR). Unfortunately, these techniques are not well suited for point-of-care application, especially in the resource-limited regions of the world, as they require highly trained personnel to perform the test, they take a long time to complete (especially culturing), and they require sophisticated lab equipment. Thus, there is a great need for simpler, faster, and more accurate methods for bacterial detection. In this thesis, we present a simple, low-cost assay for detecting pathogenic bacteria that is based on the immobilization of a bacteria-specific RNA-cleaving DNAzyme (DNAzyme) onto a surface. If the target bacteria is present, a fluorescently labelled piece of DNA (FDNA) is released through the activity of the DNAzyme; if the target bacteria is not present, the FDNA remains attached to the surface as part of the DNAzyme construct. This method allows untrained users to determine whether a target bacteria is present by simply monitoring the fluorescence intensity in the liquid phase with a hand-held fluorimeter. The first step in this work was to experimentally evaluate different surfaces (including reduced graphene oxide and different beads) onto which the DNAzyme could be immobilized. These tests determined that agarose beads, covered with streptavidin, were ideally suited for DNAzyme immobilization. Next, we conducted a comparative evaluation of the kinetics/activity of the DNAzyme that had been immobilized onto the beads and the free DNAzyme in solution; the results of this evaluation revealed virtually identical reaction rates for the two cases, suggesting no loss of activity after immobilization. Finally, we explored how the DNAzyme sequence length influenced the assay. Specifically, we analyzed a full-length DNAzyme (Full DNAzyme)

sequence and a truncated alternative (Short DNAzyme) and found that the full-length construct resulted in faster signal generation. Therefore, it was determined that the long version should be used in the assays.

When coupled with a filtration step, the immobilization of biotinylated DNAzymes onto the surface of streptavidin-coated agarose beads enabled the sensitive detection of *E. coli* in both water samples and complex matrices, such as milk and apple juice. The bead-based assay was able to produce a strong fluorescence signal readout in as little as 2.5 min following contact with *E. coli*, and it was capable of achieving a detection limit of 1,000 colony-forming units (CFUs) without sample enrichment. As DNAzyme probes can be generated through *in vitro* selection to react to different bacteria, the RNA-cleavage based detection mechanism described in this work can be adapted for the detection of a wide range of bacterial targets. Overall, this research has led to the development of a highly sensitive and easy-to-use fluorescent bacterial detection assay that is highly attractive for field applications, especially in resource-limited regions.

*To my parents for making me be who I am;*

*And to my husband for supporting me all the way.*

## **Acknowledgements**

First of all, I would like to express my special appreciation and thanks to my supervisor Dr. Carlos Filipe for the patient guidance, great support and warm-hearted advice he has provided throughout my time as his student. I have been extremely lucky to have a supervisor who cared so much about my work. The door to Dr. Filipe's office was always open whenever I ran into a trouble spot or had a question about my research or writing. It was a real privilege and an honor for me to share of his exceptional scientific knowledge but also of his extraordinary human qualities.

I have been extremely fortunate to have not only one, but two outstanding supervisors. I am greatly indebted to my co-supervisor, Dr. Yingfu Li, for his constant support, invaluable guidance, and constructive suggestions, which were determinant for the accomplishment of the work presented in this thesis. He constantly encouraged and challenged me to explore beyond my set criteria. At many stages in the course of this research project I benefited from his advice, particularly so when exploring new ideas. Dr. Li is a true inspiration on how to approach science with a lens focused on excellence, with critical thinking and with the goal of having an impact.

I am also deeply grateful to my best friends, Dr. Erin McConnell and Dr. Dingran Chang, two postdoctoral fellows in our research group, for their friendship, excellent guidance and continual helps in my project. Their advice on both research as well as on my career have been priceless. Many of the experiments would not have been completed as easily without their brilliant comments and suggestions.

I also want to thank all my lab mates for their continual support, discussions and debates which helped me to promote my knowledge in my field.

Last, but not least, I wish to express my profound gratitude and love to my parents for their endless love, wise counsel and sympathetic ear throughout my life. This accomplishment would not have been possible without them. I would also like to thank my beloved husband, Hosein, for his love and also unfailing support and continuous encouragement through the process of researching and writing this thesis. Thank you.

## Table of Contents

<b>Abstract.....</b>	<b>iii</b>
<b>Acknowledgements .....</b>	<b>vi</b>
<b>List of Figures.....</b>	<b>x</b>
<b>List of Tables .....</b>	<b>xv</b>
<b>Abbreviations .....</b>	<b>xvi</b>
<b>1. Introduction.....</b>	<b>1</b>
<b>1.1. Conventional methods for bacteria detection.....</b>	<b>3</b>
<b>1.2. Introduction to nucleic acids.....</b>	<b>6</b>
1.2.1. Functional nucleic acids .....	7
1.2.2. Discovery of DNAzymes.....	9
1.2.3. DNAzymes for bacteria detection .....	11
1.2.4. Catalytic mechanism of RNA-cleaving DNAzymes .....	12
1.2.5. Role of metal ions in RNA-cleaving DNAzyme catalysis .....	13
<b>1.3. Biosensors .....</b>	<b>15</b>
1.3.1. A brief overview of biosensors.....	15
1.3.2. Biosensors in bacteria detection .....	17
1.3.3. Fluorescent DNAzyme-based biosensors .....	19
<b>1.4. Immobilization of biomolecules on sensing interfaces.....</b>	<b>24</b>
1.4.1. An overview of biomolecules immobilization .....	24



1.4.2. DNAzyme-nanomaterial based biosensors.....	26
<b>1.5. Objective and thesis outline .....</b>	<b>28</b>
<b>1.6. References.....</b>	<b>31</b>
<b>2. Development of a bead-based assay for the detection of <i>E.coli</i> using DNAzymes .....</b>	<b>39</b>
<b>2.1. Abstract.....</b>	<b>40</b>
<b>2.2. Introduction.....</b>	<b>41</b>
<b>2.3. Results and Discussion.....</b>	<b>43</b>
2.3.1. Kinetic analysis of the Full DNAzyme’s activity in solution and immobilized on agarose beads.....	43
2.3.2. Detection sensitivity of the Full DNAzyme in solution compared to immobilized on agarose beads.....	47
2.3.3. Specificity of the Full DNAzyme in solution and immobilized on agarose beads.....	49
2.3.4. Truncation analysis of the DNAzyme in solution and immobilized on agarose beads	50
2.3.5. Performance of the Full DNAzyme immobilized on agarose beads for the detection of <i>E. coli</i> in complex sample matrices .....	52
<b>2.4. Conclusion .....</b>	<b>55</b>
<b>2.5. Materials and Methods.....</b>	<b>56</b>
2.5.1. Chemical reagents.....	56
2.5.2. Bacterial cells preparation .....	57
2.5.3. Preparation of DNAzymes.....	58

2.5.4. Immobilization of DNAszymes onto agarose beads .....	59
2.5.5. Internal normalization for calculating the amount of cleavage product .....	60
2.5.6. Kinetic analysis of the Full DNAszyme’s activity in solution.....	61
2.5.7. Kinetic analysis of the Full DNAszyme’s activity immobilized on agarose beads .....	62
2.5.8. Detection sensitivity of the Full DNAszyme in solution and immobilized on agarose beads .....	62
2.5.9. Specificity of the Full DNAszyme in solution and immobilized on agarose beads.....	63
2.5.10. Truncation analysis of the DNAszyme in solution and immobilized on agarose beads .....	63
2.5.11. Performance of the Full DNAszyme immobilized on agarose beads for the detection of <i>E. coli</i> in complex sample matrices.....	64
<b>2.6. Appendix.....</b>	<b>66</b>
<b>2.7. References .....</b>	<b>72</b>
<b>3. Conclusions and future work.....</b>	<b>76</b>
<b>3.1. Conclusions.....</b>	<b>76</b>
<b>3.2. Future work .....</b>	<b>78</b>

## List of Figures

- Figure 1.1.** (a) The chemical structure of nucleotides, and (b) the five nucleobases (A, T, C, G, U). ..... 7
- Figure 1.2.** *In vitro* selection scheme for isolating functional nucleic acids. A starting library of  $10^{14} - 10^{16}$  unique sequences is subjected to a function-based selection step in order to isolate a sequence with a desired function. During this process, inactive sequences are removed from the system, and active sequences are enriched. This process is repeated until the library is sequenced. The sequences are then chemically synthesized and tested for activity. .... 8
- Figure 1.3.** Secondary structure of the GR-5 RNA-cleaving DNAzyme. The substrate strand and the enzyme strand are shown in black and blue, respectively. The cleavage site is highlighted in red, and the arrow indicates the cleavage position. .... 10
- Figure 1.4.** Secondary structures of (a) the 10-23 DNAzyme and (b) the 8-17 DNAzyme. The substrate strand and the enzyme strand are shown in black and blue, respectively. The cleavage site is highlighted in red and the arrow indicates the cleavage position. .... 11
- Figure 1.5.** Schematic illustration of an RNA-cleaving fluorogenic DNAzyme (RFD) probe that fluoresces upon contact with live *E. coli* cells. The RFD cleaves a fluorogenic DNA substrate at a lone RNA linkage (blue R), which is flanked by two nucleotides labeled with a fluorophore (F) and a quencher (Q). Before the cleavage reaction, the RFD's fluorescence level is minimal due to the close proximity of the F and Q. Upon cleavage, the Q departs from the F, which produces strong fluorescence signal (adapted from Ref. <sup>40</sup>). .... 12

**Figure 1.6.** Scheme of the RNA cleavage reaction in which the 2'-hydroxyl group attacks the adjacent phosphodiester bond, forming 2', 3'-cyclic phosphate and 5'-hydroxyl RNA termini..... **13**

**Figure 1.7.** Potential catalytic roles of metal ions in the cleavage of a phosphodiester bond. Metal ions can act as (a) a general acid catalyst, (b) a general base catalyst, (c) a Lewis acid that stabilizes the leaving group, (d) a Lewis acid that enhances the deprotonation of the attacking nucleophile, and (e) an electrophilic catalyst that increases the electrophilicity of the phosphorus atom (adapted from Ref. <sup>45</sup>)..... **14**

**Figure 1.8.** Conceptual schematic representation of biosensors. .... **17**

**Figure 1.9.** (a) Approximate number of articles using each technique to detect and/or identify pathogenic bacteria. (b) Time series of the number of works published on pathogenic bacteria detection over the last thirty years (adapted from Ref. <sup>3</sup>). .... **17**

**Figure 1.10.** Schematic illustration of the arrangement of Fluorophore (F) and Quencher (Q) dyes on the DNAzyme. (a) F and Q placed at opposite ends of the substrate strands. (b) F and Q placed on the same side of the DNAzyme, but on different strands for closer contact quenching effects. (c) Introduction of a second Q on the other end of the substrate to reduce the background fluorescence inherent to the previous design. (d) F and Q flanking the cleavage site..... **21**

**Figure 1.11.** DNAzyme-based fluorescent biosensors. (a) DNA substrates with a fluorophore immobilized onto AuNPs for quenching. (b) A cis-conformation brings the fluorophore closer to the AuNP. (c) Many DNAzymes-substrate probes could be adsorbed onto gold nanorods for close contact quenching of the fluorophore. (d) Double-stranded DNA has limited affinity for graphene oxide and carbon nanotubes. Upon cleavage, the single-

stranded fluorescent piece will be adsorbed onto these nanomaterials and become quenched.

(e) A large ssDNA loop is introduced to keep the fluorescent probe bound to graphene oxide. Adjusting the length of the cleaved fluorescent strand allows it to depart from the graphene oxide, thus providing a fluorescent signal (adapted from Ref. <sup>84</sup>). ..... **23**

**Figure 1.12.** Schematic illustration of the DNzyme-magnetic-bead-based biosensor (adapted from Ref. <sup>102</sup>). ..... **28**

**Figure 2.1.** Kinetic analysis of Full DNzyme activity with (a)  $10^6$  *E. coli* cells and (b)  $10^4$  *E. coli* cells. The left part shows the solution-based assay and the right part shows the bead-based assay. 10% dPAGE analysis was performed for each reaction mixture, followed by fluorescence imaging with Typhoon and analysis with ImageQuant software. Cleavage product (Clv), full length DNzyme (which is uncleaved (Unclv)), and Tracer contain FAM and can be visualized via fluorescence scanning. The marker (M) is a sample of the DNzyme that has been heat treated with NaOH (at 90 °C for 5 min) in order to reveal the locations of the Clv and Unclv bands. The % Clv for each sample was calculated using the internal control, referred to as “Tracer” in the gel images (see Methods section for details). The lane of the bead-based samples, identified as “SC” in the gel images, is the Solution-Based Control (the last lane from the corresponding left part), which was added to confirm the accuracy of the calculations (see Methods section for details). NC represents the Negative Controls which are the samples that do not contain *E. coli*. (c) The bottom graph depicts the kinetic profiles associated with DNzyme activity for the solution- and bead-based assays. The data shown in this chart are the average of three independent experiments, and the error bars are based on the standard deviations of triplicate experiments. .... **45**

**Figure 2.2.** Comparison of Full DNzyme detection sensitivity in solution-based and bead-based assays over 1 hr and 12 hr incubation time. The Y-axis indicates the relative activity, which is the percentage of the ratio of the DNzyme cleavage in the bead-based assay to the DNzyme cleavage in the solution-based assay. The X-axis indicates the number of *E. coli* cells used in each reaction mixture. The data shown in the charts are the average of three independent experiments and the error bars are based on the standard deviations of triplicate experiments..... **48**

**Figure 2.3.** Specificity test of the Full DNzyme using four different bacteria. The left image shows the solution-based assay, and the right image shows the bead-based assay. EC: *Escherichia coli*; LP: *Legionella pneumophila*; LM: *Listeria monocytogenes*; BS: *Bacillus subtilis*. Clv and Unclv represent the cleavage product and the full-length DNzyme (which is uncleaved) respectively. The % Clv was calculated using the internal control, labeled “Tracer”, in the gel image (see Methods section for details). ..... **50**

**Figure 2.4.** (a) Schematics of the Full and the Short DNzyme sequences for *E.coli*. Both sequences start with 5' FAM and are modified with Biotin at 3' end of the sequences (the end point of the sequences is shown with the marker). The sequences are also provided in Supplementary Information, Table S1. (b) Truncation analysis of *E. coli* DNzyme in solution (top panel) and immobilized on agarose beads (bottom panel). Clv in the gel images represents the cleavage product. Unclv1 and Unclv2 show the Full and Short DNzymes (both uncleaved), respectively. The % Clv for each sample was calculated using the internal control, labeled “Tracer”, in the gel images (see Methods section for details). ..... **51**

**Figure 2.5.** (A) Confocal microscopy of the Full DNzyme immobilized on agarose beads. This image confirms the attachment of the biotinylated DNzyme to the surface of streptavidin-

coated agarose beads. (B) Schematic of the bead-based biosensor. (C) Performance of the bead-based biosensor in detecting *E. coli* in water, milk and apple juice samples (Water: water alone; Water+EC: water spiked with *E. coli*; Milk: diluted milk alone; Milk+EC: diluted milk spiked with *E. coli*; AJ: diluted apple juice alone; AJ+EC: diluted apple juice spiked with *E. coli*). Row 1 presents the maximum fluorescence signal obtained during in the solution-based assay for each matrix with and without *E. coli*. Row 2 presents the cleavage event signal in the bead-based assay. Row 3 shows the autofluorescence of control samples without DNAzyme and beads. Row 4 shows the autofluorescence of the control samples without DNAzyme and beads after subjection to filtration. RF is the relative fluorescence calculated for Row 1 and Row 2 by dividing the fluorescence signal of each zone by the fluorescence signal of the reaction buffer zone..... **54**

**Figure S1.** Immobilization of *E. coli* DNAzyme onto three different materials: (a) Reduced graphene oxide; (b) Magnetic beads; and (c) Agarose beads. In each gel image, the left, middle, and right columns indicate samples with no *E. coli* cells, the presence of *E. coli* K12, and the presence of *E. coli*  $\Delta$ rna (this bacteria is not a specific protein target for the DNAzyme, so it does not induce the cleavage activity of the DNAzyme). As gel images show, agarose beads yielded the highest signal-to-background ratio (comparing  $3/1.3 = 2.3$ ,  $8.3/0.5 = 16.6$ ,  $3.5/0.1 = 35$  for reduced graphene oxide, magnetic beads, and agarose beads, respectively). Note that the higher cleavage exhibited by magnetic beads was due to the higher number of *E. coli* cells (5000 *E. coli* cells) than were used with reduced graphene oxide and agarose beads (2000 *E. coli* cells)..... **67**

**Figure S2.** Differences between previously reported *E. coli* DNAzyme and our probe. (a) The previously reported *E. coli* DNAzyme was ligated to the FQ substrate at its 3' end<sup>40</sup>. (b) Also

previously investigated, the DNAzyme was ligated to the FQ substrate at its 5' end <sup>26</sup>. (c) The DNAzyme was ligated to the FAM-labeled substrate at its 5' end (internal modification). (d) The DNAzyme was ligated to the FAM-labeled substrate at its 5' end (external modification). The aforementioned probe for *E. coli* was used in this work because it resulted in the best cleavage activity. *Bacillus subtilis* bacterium (*B. sub*) was used as the control in each experiment. .... **68**

**Figure S3.** 10% dPAGE analysis of sensitivity test for creating Figure 2.2. (a) Solution-based assay, 1 hr incubation time. (b) Bead-based assay, 1 hr incubation time. (c) Solution-based assay, 12 hr incubation time. (d) Bead-based assay, 12 hr incubation time. (e) Similar experiment using  $10^7$  *E. coli* cells. S-b and B-b represent the solution-based and bead-based assays, respectively. The % Clv for each sample was calculated using the internal control, which is labeled, “Tracer”, in the gel images (see Methods section in the main text for details). .... **69**

**Figure S4.** Autofluorescence signal of the controls, and the fluorescence signals of the reaction mixtures represented in Figure 2.5c. EC stands for *E. coli*, and the reaction mixtures are defined in the legend of Figure 2.5. The error bars are based on the standard deviations of the experiments, which were performed in triplicate. .... **70**

**List of Tables**

**Table S1.** The sequences of and modifications to all oligonucleotides used in this work. .... **71**



## Abbreviations

ATP	Adenosine 5'-Triphosphate
AuNPs	Gold Nanoparticles
BS	<i>Bacillus Subtilis</i>
CEM	Crude Extracellular Mixtures
CIM	Crude Intracellular Mixtures
CNTs	Carbon Nanotubes
ddH <sub>2</sub> O	Double-Deionized Water
DNA	Deoxyribonucleic Acid
DNAzyme	Deoxyribonucleic Acid Enzyme
dPAGE	Denaturing Polyacrylamide Gel Electrophoresis
dsDNA	Double-stranded DNA
E. coli	<i>Escherichia Coli</i>
EDTA	Ethylene Diamine Tetraacetic Acid
FNA	Functional Nucleic Acid
GNRs	Gold Nanorods
GO	Graphene Oxide
LM	<i>Listeria Monocytogenes</i>

LOD	Limit of Detection
LP	<i>Legionella Pneumophila</i>
PNK	T4 Polynucleotide Kinase
QB	Quenching Buffer
RB	Reaction Buffer
RCA	Rolling Circle Amplification
RFD	RNA-cleaving Fluorogenic DNazymes
RNA	Ribonucleic Acid
SELEX	Systematic Evolution of Ligands by Exponential Enrichment
ssDNA	Single-stranded DNA

## 1. Introduction

Pathogenic bacteria are a leading cause of illness and death in the developing world and rural areas in the developed world, largely due to lack of infrastructure and resources <sup>1</sup>. Since pathogens can be transmitted via plants, animals, and humans, it is easy for infectious diseases to spread exponentially, which can reach pandemic levels if left unchecked <sup>2</sup>. Although early diagnosis is the most effective method for preventing the spread of infectious diseases, it can be challenging to do so using conventional methods due to the need for expensive equipment, specialized sample preparation, and slow data output <sup>2</sup>. Fortunately, the development of modern biosensors has enabled these obstacles to be overcome, particularly the creation of miniaturized devices that are capable of providing simple, rapid output that can be analyzed at the point-of-care without any specialized training <sup>3-5</sup>.

In addition to point-of-care diagnostics and early treatment of infectious diseases in humans, the detection of microbial pathogens is also a key concern at various levels of the food industry <sup>6</sup>, in water and environmental quality control <sup>7</sup>, and in clinical diagnoses <sup>8</sup>. Thus, there is a significant need for simple methods that are capable of rapidly detecting known pathogens, as well as new platforms that can be quickly put in place to create assays for new pathogens during unanticipated outbreaks.

The overall objective of this work was to develop a biosensor that uses DNAzymes to detect pathogenic bacteria. Specifically, this research aimed to develop a sensitive, easy-to-use, low-cost fluorescent bead-based assay for the detection of *Escherichia coli* (*E. coli*), which was selected as the model bacterium for this work. The molecular recognition element in this method

is a bacteria-specific RNA-cleaving DNAzyme probe that reports the presence of a target bacterium by generating a fluorescence signal. The bead-based assay described in this work, coupled with a simple partitioning step, enabled the sensitive detection of *E. coli* in both water and complex matrices, such as milk and apple juice. It is worth noting that DNAzyme probes can be isolated through *in vitro* selection to react to different bacteria. Thus, while the current study uses an *E. coli*-specific DNAzyme for the detection of *E. coli*, the proposed bead-based assay could be easily used to detect a wide range of bacterial targets by utilizing the appropriate DNAzyme.

This chapter discusses recent advances in biosensor development and introduces DNAzyme-based sensors as reliable probes that can be used in biosensing devices for bacterial detection. Chapter two opens with a discussion of the three materials that were examined for *E. coli*-specific DNAzyme immobilization: reduced graphene oxide, magnetic beads, and agarose beads. Agarose beads were ultimately selected for this research, as they produced the highest signal-to-background ratio. Next, Chapter two details a comprehensive study that compared how *E. coli*-specific DNAzymes behave when they are immobilized on agarose beads or are free in solution in order to determine whether agarose beads can be used as solid support in the development of an *E. coli*-detection biosensor. Finally, Chapter Two documents the bead-based assay's ability to detect *E. coli* in both water samples and complex sample matrices, such as milk and apple juice. As the results show, the proposed bead-based assay was able to successfully decrease the non-specific background noise by using a simple partitioning step, which in turn allowed for the sensitive detection of *E. coli*. These advantages, combined with the biosensor's

high stability and specificity, make the proposed bead-based bacterial-detection assay highly attractive for field applications, especially in resource-limited regions.

### **1.1. Conventional methods for bacteria detection**

Bacterial infection linked to contaminated food and water causes millions of deaths annually, particularly in the developing world where routine testing is currently not possible<sup>9-11</sup>. Thus, safety concerns related to the bacterial contamination of drinking water and food have attracted increasing attention worldwide, and this has led to efforts to improve technologies for detecting such pathogens, clinically diagnosing infection, and health surveillance in general<sup>12,13</sup>. Currently, conventional methods for pathogen detection can be roughly divided into three categories: culture and colony counting, immunological assays, and polymerase chain reaction (PCR)-based methods<sup>14</sup>. These methods offer high sensitivity and specificity, and they are able to provide both quantitative and qualitative information, which is often a necessity. However, they are also hampered by some key drawbacks. The most significant of these drawbacks is the need for relatively long processing times, which is a clear indication that better solutions are needed.

Colony counting is widely considered to be the gold standard for pathogen-detection applications ranging from clinical diagnosis to food safety<sup>3,14,15</sup>. This process involves isolating and growing a suspect pathogen, and then visually inspecting it. Due to the inherent amplification during colony growth, this method is good for identifying very low amounts of organisms (i.e. single cells). Unfortunately, this technique requires lengthy turn-around times for results due to long incubation periods and the need for intensive labor. For example,

depending on the pathogen, initial results often require at least 2 days, with confirmation only being possible after 7-10 days <sup>14,15</sup>. Furthermore, colony counting methods require the use of culturable pathogen, which may not always be possible due to stringent environmental or nutritional requirements.

Immunological assays are commonly used for pathogen detection for their ability to be adapted to a wide variety of pathogens, including bacteria and viruses. The enzyme-linked immunosorbent assay (ELISA) method is an example of a well-known immunological assay. Immunological assays rely on using antibodies to recognize antigens and other biomolecules specific to a given target. With some notable exceptions, such as toxins, antibodies can be developed for an arbitrary target. The primary advantage of using immunological assays over colony counting approaches is their ability to provide reduced assay times while still maintaining high specificity. Furthermore, ELISA's ability to provide an optical response has led to it being widely deployed in clinical laboratories through the use of commercially available ELISA kits. Despite these advantages, immunological assays still suffer from a number of drawbacks, including insufficient sensitivity to detect bacterial cells at low concentrations, the need for multiple steps to retrieve antigens from cells, highly trained personnel, and several hours of runtime to produce results <sup>3,16</sup>. Moreover, antibody isolation is costly and difficult to scale up for mass production <sup>17</sup>.

PCR-based methods comprise a wide variety of detection schemes that use nucleic acid amplification to increase the concentration of a detection target. The amplification of target deoxyribonucleic acid (DNA) sequences lends conventional PCR-based methods a high degree

of sensitivity and even allows them to detect single gene copies. Furthermore, it is important to note that, unlike colony counting, this sensitivity is achieved without a prolonged incubation time, as these methods do not require bacteria to be grown <sup>16</sup>. Specificity is achieved through the use of primers and probes that are designed to target sequences that are unique to the pathogen of interest. However, interference from non-pathogenic genetic material may lead to misleading results due to mismatching or non-specific amplification, which means that precise genetic information is required in order to ensure confidence in the results <sup>14,16</sup>. Following target amplification, samples are traditionally separated by gel electrophoresis, but this approach requires complex sample preparation procedures and manipulations that can increase labor costs and processing times <sup>3</sup>. Fortunately, newer technologies such as real-time PCR and fluorescent molecular probes have been designed to mitigate these challenges. Perhaps the main drawback of traditional PCR-based methods is their inability to distinguish between viable and non-viable cells. This deficiency is due to the fact that both viable and non-viable cells contain the amplification target, which often yields false-positive results <sup>14</sup>. To address this issue, assays have been developed that employ reverse transcription PCR (RT-PCR) to target rapidly deteriorating messenger ribonucleic acid (mRNA) strands that are present during the cell's growth cycle <sup>14,18</sup>. Overall, the number of limitations inherent to traditional bacteria detection methods demonstrates the importance of developing new, particularly simpler, methods for detecting bacterial pathogens.

Over the past decade, many attempts have been made to use biosensor technology to provide sensitive and reliable bacteria detection <sup>19</sup>. Biosensors offer a number of advantages,

such as the elimination or simplification of the sample preparation steps and high specificity and sensitivity, which enables a broad spectrum of analytes to be detected in complex sample matrices. Thus far, one common approach to employing this technology has been to use antibodies as recognition elements in biosensor systems<sup>20</sup>. DNAzymes are remarkable candidates for these types of sensing applications because they offer several advantages, which will be discussed in this chapter. DNAzymes or deoxyribozymes are chemically synthesized single-stranded DNA molecules that exhibit high chemical stability, as well as excellent recognition specificity and affinity for their targets, which makes them an ideal candidate for use in biosensor development. Therefore, this thesis will focus on the DNAzyme-based biosensors for use in the detection of bacterial pathogens.

The field of biosensor research has been extremely fruitful and has given rise to a multi-billion dollar industry. DNAzyme-based biosensors have emerged as a new option in the field of diagnostics, and they have the potential to further contribute to this exciting subject. In the following sections, DNAzymes and their applications in biosensor development will be introduced, before turning the discussion to current trends, progress, and deficiencies in current biosensors technology, and how these deficiencies can be resolved using DNAzymes.

## **1.2. Introduction to nucleic acids**

Nucleic acids are biopolymers that take their name from their location: the nucleus of a cell<sup>21</sup>. These polymers are made up of monomers called nucleotides, which are in turn made up of three parts: a) a pentose sugar, namely ribose or 2'-deoxyribose; b) a heterocyclic base—either be a purine (two-carbon nitrogen ring base) or a pyrimidine (one-carbon nitrogen ring base)—



which is linked to the 1'-carbon on the sugar ring; and c) a phosphate group at the 5'-carbon (Figure 1.1 a)<sup>21</sup>. Deoxyribonucleic acid (DNA) and ribonucleic acid (RNA) are the two types of nucleic acids found in nature, and they differ from each other based on their pentose sugar (2'-deoxyribose in DNA and ribose in RNA) and one base that is unique to each (thymine (T) in DNA and uracil (U) in RNA)<sup>21</sup>. Despite being differentiated by a difference in one base, RNA and DNA still share three common bases: adenine (A), guanine (G), and cytosine (C) (Figure 1.1 b)<sup>21</sup>. Another difference between RNA and DNA is that RNA is usually single-stranded whereas DNA features a double-stranded helical structure that is held together by two hydrogen bonds between A and T and three hydrogen bonds between G and C<sup>21</sup>. In terms of function, DNA is responsible for carrying genetic information and transcribing it into RNA, which in turn takes this information and translates it into proteins.

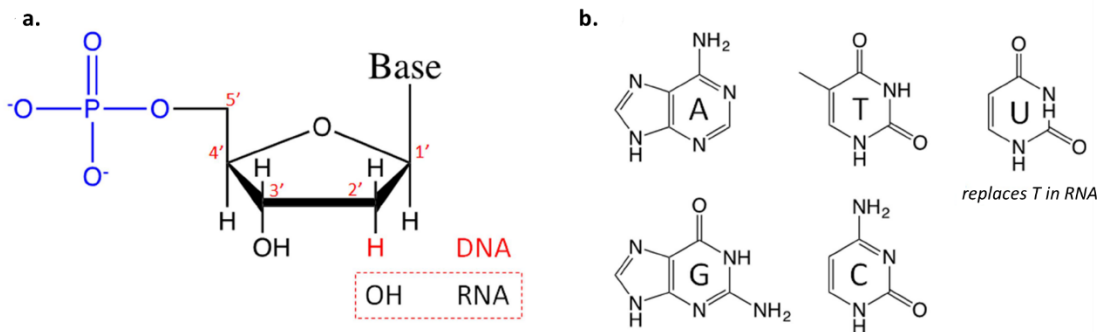


**Figure 1.1.** (a) The chemical structure of nucleotides, and (b) the five nucleobases (A, T, C, G, U).

### 1.2.1. Functional nucleic acids

Over the last thirty years a number of discoveries have demonstrated that, in addition to being genetic material carriers, nucleic acids can perform active roles in binding and catalysis,

thus resulting in the term, “Functional Nucleic Acids”<sup>22,23</sup>. This finding has opened doors to a new research paradigm in nucleic acid chemistry and biology.

In the 1990s, pioneering research for probing DNA or RNA molecules that can serve purposes beyond information storage has led to the development of a technique known as *in vitro* selection, or SELEX (Systematic Evolution of Ligands by Exponential Enrichment)<sup>24,25</sup>. It is a combinatorial approach that begins with a large randomized library of  $10^{14}$  -  $10^{16}$  DNA or RNA molecules. In *in vitro* selection, these pools of sequences are subjected to successive rounds of selection and amplification; in each round, sequences expressing the desired function are enriched, while those that do not are discarded (Figure 1.2). This “test-tube evolution” approach will tend to produce synthetic molecules that can act as molecular receptors or catalyze chemical reactions. These unique molecules, known as “Functional Nucleic Acids” (FNAs), are capable of detecting a wide range of targets, from small molecules, to proteins, to whole cells<sup>26</sup>.

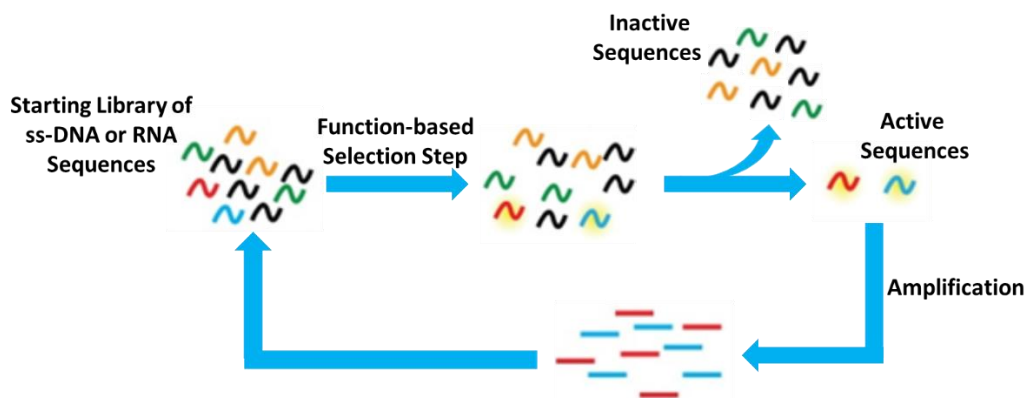


**Figure 1.2.** *In vitro* selection scheme for isolating functional nucleic acids. A starting library of  $10^{14}$  –  $10^{16}$  unique sequences is subjected to a function-based selection step in order to isolate a sequence with a desired function. During this process, inactive sequences are removed from the system, and active sequences are enriched. This process is repeated until the library is sequenced. The sequences are then chemically synthesized and tested for activity.

### 1.2.2. Discovery of DNAzymes

The use of *in vitro* selection led to the discovery of a new class of functional nucleic acids: DNAzymes, or deoxyribozymes<sup>24</sup>. These nucleic acids are single-stranded DNA molecules that are capable of catalyzing chemical reactions, such as RNA cleavage<sup>23</sup>, DNA cleavage<sup>27</sup>, DNA ligation<sup>28</sup>, DNA phosphorylation<sup>29</sup>, DNA deglycosylation<sup>30</sup>, and porphyrin metalation<sup>31</sup>. Furthermore, DNAzymes can be isolated to recognize a wide range of target analytes including metal ions, proteins, and even whole cells through *in vitro* selection<sup>26</sup>. Unlike its counterpart, ribozyme, which is a naturally-occurring RNA molecule that is capable of catalyzing specific chemical reactions<sup>32</sup>, all DNAzymes reported to date have been selected artificially; that is, no examples of DNAzymes have been found in biological systems. The first DNAzyme, known as GR-5, was discovered in 1994 by Breaker and Joyce<sup>23</sup>. Figure 1.3 shows the secondary structure of the GR-5 DNAzyme. The top strand (denoted in black) is the substrate strand, which is made up entirely of DNA nucleotides and one ribo-adenosine (rA labeled in red) in the middle. This ribo-adenosine molecule serves as the RNA cleavage site. Below the substrate strand is the enzyme strand, which has a catalytic core consisting of 15 single-stranded nucleotides (labeled in blue) that are flanked by two base-pairing regions (labeled in green)<sup>23</sup>. GR-5 catalyzes the RNA cleavage reaction in the presence of  $Pb^{2+}$ , with a catalytic rate of around  $1 \text{ min}^{-1}$  at  $23^{\circ}\text{C}$  and a pH of 7. This rate is about  $10^5$  times higher than the uncatalyzed reaction under the same conditions<sup>23</sup>.

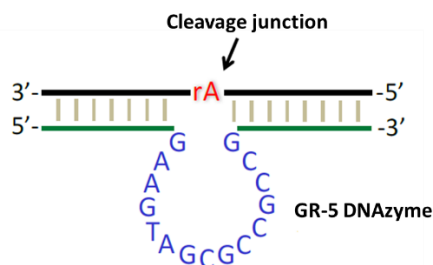


**Figure 1.3.** Secondary structure of the GR-5 RNA-cleaving DNAzyme. The substrate strand and the enzyme strand are shown in black and blue, respectively. The cleavage site is highlighted in red, and the arrow indicates the cleavage position.

Since the discovery of GR-5, many other RNA-cleaving DNAzymes have been successfully isolated. Of these newly discovered RNA-cleaving DNAzymes, 10-23 and 8-17, which were first reported by Santoro and Joyce in 1997<sup>33</sup>, have been the most studied, widely used, and isolated via *in vitro* selection (Figure 1.4). The 10-23 and 8-17 DNAzymes take their names from the round and clone number in their respective selections, with both being relatively small motifs.

The 10-23 DNAzyme was isolated through *in vitro* selection under simulated biological conditions (150 mM KCl, 2 mM MgCl<sub>2</sub>, 50 mM Tris buffer, pH 7.5, 37°C)<sup>33</sup>. As shown in Figure 1.4 a, its catalytic domain is composed of 15 nucleotides (labeled in blue)<sup>33</sup>. In addition, the 10-23 DNAzyme's catalytic activity is Mg<sup>2+</sup>-dependent with a rate of ~0.1 min<sup>-1</sup> in the presence of 2 mM Mg<sup>2+</sup>. By changing the substrate-binding domain, this DNAzyme can be used to target various RNA substrates.

The 8-17 DNAzyme was also isolated from the same selection procedure<sup>33</sup>. As shown in Figure 1.4 b, this DNAzyme has a relatively small catalytic core consisting of a stem-loop of 3-base pairs and 9 conserved nucleotides (labeled in blue). Unlike the 10-23 DNAzyme, the 8-17

DNAzyme is substantially more active with  $\text{Pb}^{2+}$  than other metal ions, although moderate activity can still be observed in the presence of many other divalent ions (e.g.,  $\text{Zn}^{2+}$ ,  $\text{Ca}^{2+}$ ,  $\text{Mg}^{2+}$ ,  $\text{Mn}^{2+}$ , and  $\text{Co}^{2+}$ ). As a consequence, this DNAzyme has been frequently isolated from other subsequent *in vitro* selections<sup>34–36</sup>.

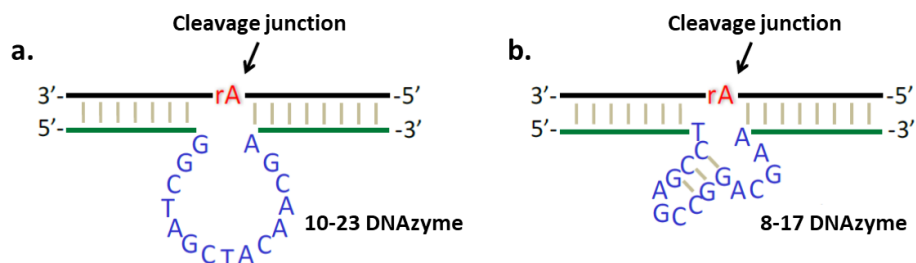


**Figure 1.4.** Secondary structures of (a) the 10-23 DNAzyme and (b) the 8-17 DNAzyme. The substrate strand and the enzyme strand are shown in black and blue, respectively. The cleavage site is highlighted in red and the arrow indicates the cleavage position.

### 1.2.3. DNAzymes for bacteria detection

RNA-cleaving DNAzymes have proven to be particularly useful in developing detection methods for a wide variety of targets<sup>37,38</sup>. Recently, researchers successfully used *in vitro* selection to generate RNA-cleaving fluorogenic DNAzymes (RFDs) for the real-time detection of specific bacteria<sup>39,40</sup>. The Li group was the first to isolate a DNAzyme for bacterial detection capable of cleaving a fluorogenic substrate predeposited with a fluorophore and a quencher flanking the cleavage site<sup>39</sup>. Li et al. performed 20 rounds of selection in order to isolate a highly sensitive and selective fluorogenic DNAzyme probe for *Escherichia coli* (*E. coli*) that could detect a single live cell and cleave a fluorogenic DNA substrate at a single ribonucleotide embedded in the DNA substrate. The cleavage junction of the DNA substrate is surrounded by two nucleotides, which are separately modified by a fluorophore (F) and a quencher (Q). Thus,

the substrate possesses a minimal fluorescence signal before the cleavage reaction, which indicates that no target bacteria is in contact with the DNAzyme. When the substrate is cleaved by the DNAzyme in the presence of the target bacterium, the fluorophore and the quencher separate from each other, significantly increasing the fluorescence intensity. Figure 1.5 illustrates the RFD's response to the model bacterial pathogen, *E.coli*, within the crude extracellular mixture (CEM) and the crude intracellular mixture (CIM)<sup>39</sup>. Since *in vitro* selection can be used to generate DNAzyme probes that will react to a certain bacteria, this concept can easily be extended to detect a wide range of bacterial targets by simply isolating the appropriate DNAzyme.

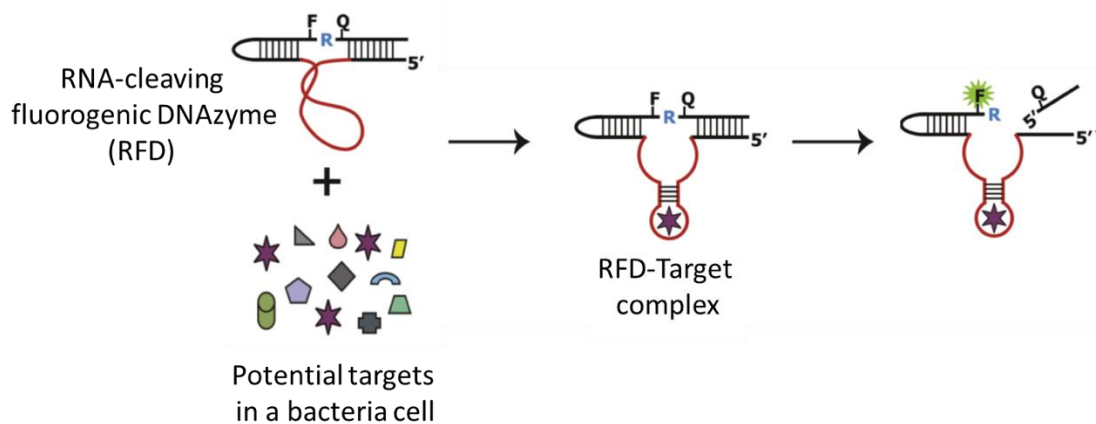


**Figure 1.5.** Schematic illustration of an RNA-cleaving fluorogenic DNAzyme (RFD) probe that fluoresces upon contact with live *E. coli* cells. The RFD cleaves a fluorogenic DNA substrate at a lone RNA linkage (blue R), which is flanked by two nucleotides labeled with a fluorophore (F) and a quencher (Q). Before the cleavage reaction, the RFD's fluorescence level is minimal due to the close proximity of the F and Q. Upon cleavage, the Q departs from the F, which produces strong fluorescence signal (adapted from Ref.<sup>40</sup>).

#### 1.2.4. Catalytic mechanism of RNA-cleaving DNAzymes

RNA-cleaving DNAzymes cleave at a single ribonucleotide within the substrate strand by prompting the 2'-hydroxyl group to initiate a nucleophilic attack on the adjacent phosphodiester

bond (Figure 1.6) <sup>41</sup>. As a genetic material, the DNA duplex is structurally inflexible; therefore, the single-stranded catalytic core is responsible for the enzymatic activity that binds functional groups to form tertiary structures. In addition, most DNAzymes are metal-assisted, which means that they require metal ions (e.g., divalent cations) as cofactors in order to achieve an appreciable reaction rate <sup>42-44</sup>. Ultimately, the substrate strand splits at the cleavage site, resulting in a 2', 3'-cyclic phosphate terminus for the 5'-fragment, and a 5'-hydroxyl RNA terminus for the 3'-fragment.

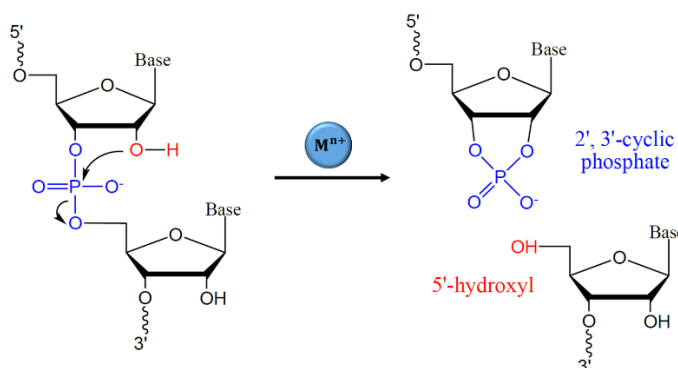


**Figure 1.6.** Scheme of the RNA cleavage reaction in which the 2'-hydroxyl group attacks the adjacent phosphodiester bond, forming 2', 3'-cyclic phosphate and 5'-hydroxyl RNA termini.

### 1.2.5. Role of metal ions in RNA-cleaving DNAzyme catalysis

Metal ions play a critical role in DNAzyme catalysis, as many DNAzymes have high binding affinities and specificities toward various metal ions. Since DNA is a negatively charged polyelectrolyte, DNA folding will strongly depend on electrostatics. As such, the presence of metal ions can effectively push the RNA cleavage reaction forward by stabilizing the negatively charged molecules <sup>45</sup>. In other words, cations may significantly promote the formation of the DNAzyme structure <sup>46</sup>. On the other hand, metal ions can serve as catalytic cofactors by directly participating in the chemical reaction <sup>45</sup>.

Figure 1.7 summarizes some of the roles that a metal ion (with  $Mg^{2+}$  as an example) can play when it directly participates in the catalysis of the RNA cleavage reaction. Figure 1.7(a) demonstrates how the proton from a metal-bound water molecule can act as a general acid catalyst for stabilizing the negative charge of the 5'-oxygen leaving group. In contrast, Figure 1.7(b) shows how a metal hydroxide ion can act as a general base catalyst that attracts the proton in order to assist with the deprotonation of the 2'-OH. Furthermore, Figure 1.7(c) demonstrates how a metal ion can function as a Lewis acid in order to stabilize the 5'-oxygen leaving group's negative charge. Similarly, as shown in Figure 1.7(d), a metal ion can act as a Lewis acid to accelerate the deprotonation of 2'-OH by coordinating directly with the 2'-oxygen. Finally, Figure 1.7(e) illustrates how a metal ion, functioning as an electrophilic catalyst, might make the phosphorus center more accessible for a nucleophilic attack by coordinating with the non-bridging oxygen atoms. As these examples show, metal ions can facilitate RNA cleavage in many different ways.

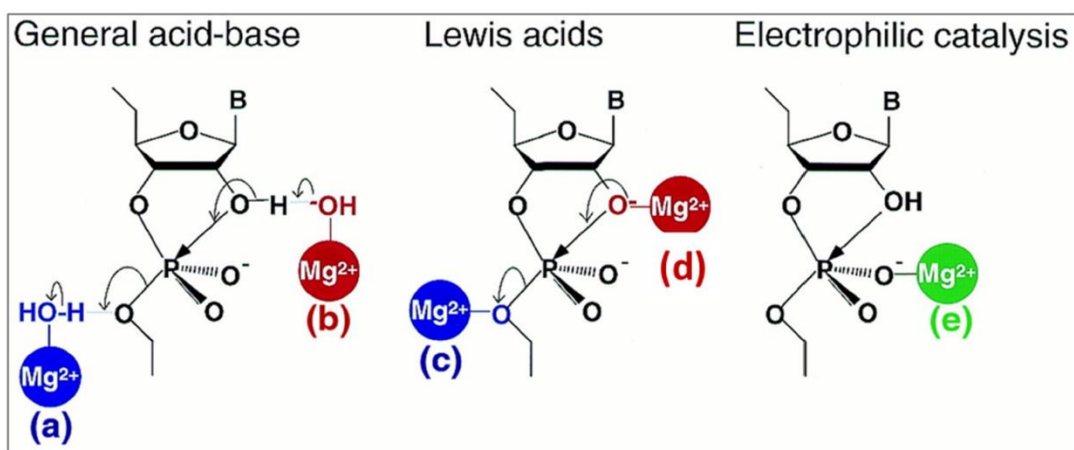


**Figure 1.7.** Potential catalytic roles of metal ions in the cleavage of a phosphodiester bond. Metal ions can act as (a) a general acid catalyst, (b) a general base catalyst, (c) a Lewis acid that stabilizes the leaving



group, (d) a Lewis acid that enhances the deprotonation of the attacking nucleophile, and (e) an electrophilic catalyst that increases the electrophilicity of the phosphorus atom (adapted from Ref. <sup>45</sup>).

### **1.3. Biosensors**

The following sections of this chapter will outline recent advances and existing deficiencies in biosensor technology, and how DNAzymes can be utilized to overcome them.

#### **1.3.1. A brief overview of biosensors**

A biosensor is an analytical device that uses a biological element in order to detect a specific analyte <sup>47</sup>. The first biosensor, which was developed by Leland C. Clark in 1956, was designed to detect oxygen. Given Clark's status as the 'father of biosensors,' it is natural that his oxygen electrode is known as the 'Clark electrode' <sup>48</sup>. In 1962, Clark would demonstrate an amperometric enzyme electrode for detecting glucose, which was followed by Guilbault and Montalvo Jr.'s unveiling of the first potentiometric biosensor for detecting urea in 1969 <sup>49</sup>. This technology would be made commercially available by the Yellow Springs Instrument Company in 1975. In 1987, this technology was brought to market by Medisense in the form of a personal point-of-care device called the "ExacTech Glucose Meter" <sup>50</sup>. Thirty years later, glucose biosensor systems have become staple point-of-care devices and account for the largest share of the biosensor market <sup>51</sup>.

The next generation of biosensor development resulted in the advent of bioaffinity sensors <sup>51</sup>. Although more costly, these immunosensors are also more sophisticated, as they function by coupling optical transducers with antibodies. As the development of biosensors accelerated, two broad categories began to emerge: 1) simple biosensors, which were primarily portable devices that could be operated by non-specialists; and 2) complex biosensors, which

were mainly highly sensitive instruments used for screening. Simple biosensors, such as the ExacTech Glucose Meter, tend to sacrifice sensitivity and throughput in favor of reducing cost, complexity, and size, while ensuring the ability to handle the chemical and biological variability of real world samples. Conversely, complex biosensors, such as immunosensors, are designed for laboratory use where factors such as sensitivity, applicability to specialized usage scenarios, and the ability to process large amounts of samples are far more important than ease-of-use and cost. Undoubtedly, the inventions of the enzyme electrode and the immunosensor represented a tremendous contribution not only in the development and success of biosensor technology, but also in capturing the attention of major diagnostic companies.

Although the biosensors have drastically expanded in terms of use and sophistication over the past 50 years, the main concept has remained the same. As shown in Figure 1.8, all biosensors are composed of two basic components: a molecular recognition element that can selectively bind to target analytes, and a transducer component that can translate recognition events into a detectable signal. Although the range of usable recognition elements was originally limited to protein enzymes and antibodies, it has since expanded to include nucleic acids, bacterial cells, and even whole tissues, thus increasing the variety and complexity of analytes that can be detected <sup>52-54</sup>. Ideally, a recognition element will have high affinity, high specificity, a wide dynamic range, a fast response time, and a long shelf life. The transduction elements in biosensors have also seen considerable innovation, particularly in terms of expanding the range of generated response signals. While biosensors were originally limited to electric signals, their

modern-day counterparts feature an assortment of output signal types, such as fluorescent, optical, and thermal signals<sup>55-58</sup>.

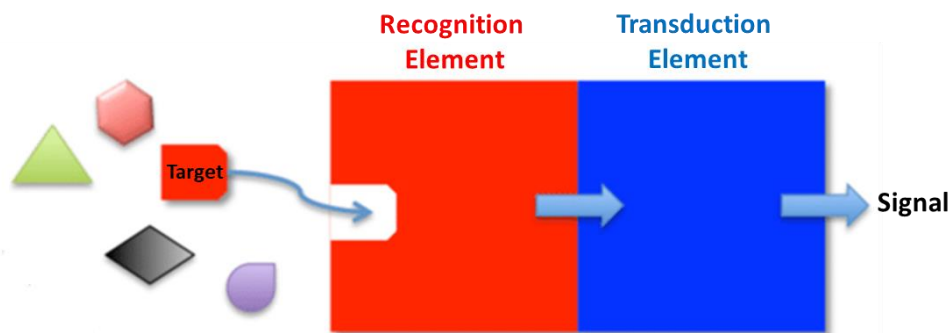


**Figure 1.8.** Conceptual schematic representation of biosensors.

### 1.3.2. Biosensors in bacteria detection

Over the past decade, many researchers have attempted to use biosensor technology as a sensitive and reliable detection protocol for overcoming the aforementioned limitations of traditional bacteria detection methods<sup>19</sup>. Figure 1.9a illustrates how often various methods are used for pathogenic bacteria detection based on their use in related studies over the past thirty years<sup>3</sup>. Although biosensor technology was the fourth most commonly used approach for pathogen detection over this thirty year period, it is also the fastest growing (Figure 1.9b)<sup>3</sup>.

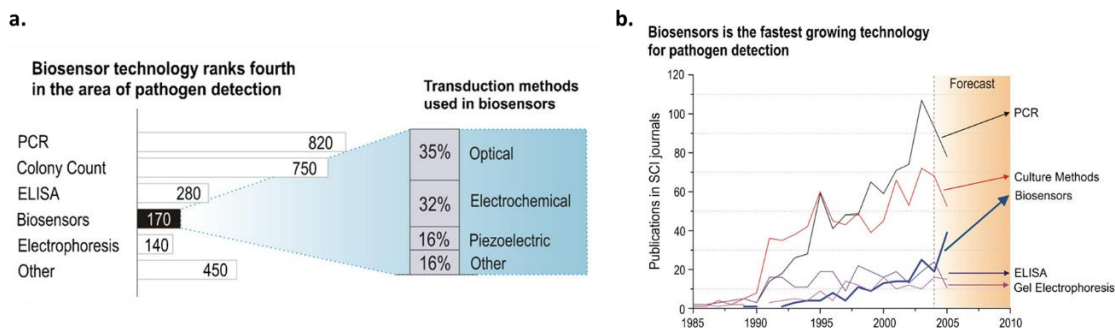


**Figure 1.9.** (a) Approximate number of articles using each technique to detect and/or identify pathogenic bacteria. (b) Time series of the number of works published on pathogenic bacteria detection over the last thirty years (adapted from Ref.<sup>3</sup>).

Biosensors' high specificity and sensitivity, in addition to their ability to eliminate or simplify the sample preparation steps, make them particularly suitable for detecting a wide range of analytes in complex matrices. Furthermore, the current interest in biosensor technology may also be due to this technology's ability to provide results that are just as reliable as those of traditional bacteria detection methods (PCR, culture methods) in much shorter times.

Thus far, protein enzymes or antibodies have been generally used as the biological recognition element in biosensor systems, and this approach appears to continue to dominate the development of new biosensors<sup>20</sup>. However, the use of protein enzymes and antibodies comes with limitations. For example, since protein enzymes are naturally evolved catalysts that are limited to a target ligand, they offer little flexibility for use in biosensors for detecting analytes without a known natural binding enzyme. In contrast, with some notable exceptions, such as toxins, antibodies offer more flexibility in this regard, and can be developed for nearly any target analyte; however, antibody isolation is also costly and difficult to scale up for mass production<sup>17</sup>. Even with the advances that have been made to enhance stability, reduce costs, and optimize the production of protein-based biosensors, there remains a need for alternative biological platforms that could fulfill the demands of this rapidly growing sector. One such alternative is Functional Nucleic Acids. Although FNA-based biosensors are still in their infancy, researchers are beginning to understand how FNAs can be manipulated and modified in order to engineer the ideal biosensor.

### 1.3.3. Fluorescent DNzyme-based biosensors

DNzymes are an important type of functional DNA that possess two unique properties: target recognition and cleavage ability. These properties allow DNzymes to be used as recognition elements in place of protein enzymes or antibodies. In addition, there are several other reasons why researchers have been increasingly focusing on DNzymes for biosensor development. Firstly, DNzymes can be isolated through *in vitro* selection to detect essentially any target of choice, including targets for which it is difficult to obtain antibodies, such as toxic metal ions and molecules with poor immunogenicity. Secondly, DNzymes are well-suited for biosensor development due to their high sensitivity, high selectivity, and their ability to efficiently detect bacteria in real time<sup>59</sup>. Thirdly, DNzymes are chemically synthesized. This is significant, as the chemical synthesis process is readily scalable, produces excellent batch-to-batch consistency, and eliminates biological contamination from viruses and bacteria. Moreover, this process allows DNzymes to be chemically modified in order to enhance their stability and bioavailability. Furthermore, the introduction of functional groups also enables interesting conjugation chemistries, such as linking nucleic acids to small molecules (dyes, carbohydrates, and amino acids), proteins, and various nanomaterials. Finally, DNzymes are stable at high temperatures and can be refolded into their native structure, and maintain their activity. Undoubtedly, the flexibility afforded by these features has been highly attractive to researchers, and they have provided the principal motivation behind the development of many innovative DNzyme-based biosensors<sup>22,60–62</sup>.

A typical RNA cleavage reaction is initiated by annealing the DNAzyme to the substrate sequence. In the presence of a target analyte, the hybridized substrate is cleaved into two fragments, which results in the departure of two strands from the DNAzyme. This reaction provides a unique opportunity to strategically position fluorophore (F) and quencher (Q) dyes, thus creating a fluorescent-based biosensor. Fluorescence is an excellent signal transduction mechanism for nucleic acids due to its high sensitivity and ease of chemical incorporation. The judicious positioning of the F and Q was investigated as shown in Figure 1.10. In order to maximize the fluorescence signal and decrease background noise, the design of F and Q underwent several evolutions. Good quenching efficiency requires the fluorophore and the quencher to be within a certain proximity from one another, which is determined by the DNAzyme's secondary structure. This requirement serves to limit the design of the DNAzyme. At first, the F and Q dyes were placed on the opposite end of the substrate strand (Figure 1.10a),<sup>63,64</sup> but this approach yielded high background fluorescence and poor signal enhancement. In order to reduce background fluorescence, the distance between F and Q was shortened by setting them on the same side of the DNAzyme, but on different strands (Figure 1.10b)<sup>65,66</sup>. This design approach was used to develop a  $\text{Pb}^{2+}$  sensor with low background fluorescence at 4 °C;<sup>66</sup> however, this approach has proven limited, as high background fluorescence can still be observed at higher temperatures if the substrate and DNAzyme strands are not efficiently hybridized. In order to improve this design, a second quencher was added to the opposite end of the substrate strand (Figure 1.10c)<sup>67</sup>. This configuration ensures that the substrate sequence will be partially quenched and the fluorescent background will remain very low, even if the two

strands dissociate or are unable to anneal correctly. This system was successfully utilized for the detection of  $\text{UO}_2^{2+}$  <sup>68</sup>. Another design that has been used to maximize signal enhancement has been to situate the fluorophore and the quencher such that they are flanking the cleavage site (Figure 1.10 d) <sup>69-71</sup>. Although the DNAzyme's cleavage activity can potentially be disturbed by inserting F and Q so close to the cleavage site, this issue can be avoided by incorporating the two dyes directly into the *in vitro* selection process. The Li group was the first to isolate a DNAzyme capable of cleaving a substrate predeposited with an F-Q pair close to the cleavage site for the purpose of bacterial detection <sup>39</sup>. This DNAzyme possessed a catalytic rate of  $7 \text{ min}^{-1}$ , which places it as one of the fastest RNA-cleaving DNAzymes known to date. Since the Li group's discovery, *in vitro* selection has been used to isolate a number of other DNAzymes capable of cleaving this fluorogenic substrate that exhibit optimal activity at varying pH levels <sup>72-74</sup>.

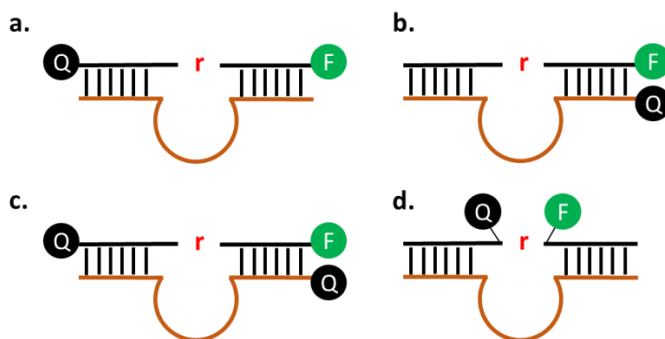


**Figure 1.10.** Schematic illustration of the arrangement of Fluorophore (F) and Quencher (Q) dyes on the DNAzyme. (a) F and Q placed at opposite ends of the substrate strands. (b) F and Q placed on the same side of the DNAzyme, but on different strands for closer contact quenching effects. (c) Introduction of a second Q on the other end of the substrate to reduce the background fluorescence inherent to the previous design. (d) F and Q flanking the cleavage site.

DNAzyme-based fluorescent sensors that use organic molecules as quenchers frequently suffer from incomplete fluorescence quenching due to poor quencher dye placement. This results

in decreased signal enhancement and increased background fluorescence. In order to overcome this issue, researchers have explored the use of gold nanoparticles (AuNPs), gold nanorods (GNRs), carbon nanotubes (CNTs), and graphene oxide (GO) as fluorescence quenchers in sensor design. For example, Chung's group immobilized a thiolated fluorescein-labeled substrate on AuNPs and observed that the fluorophore was nearly 100% quenched (Figure 1.11a). This strategy proved capable of detecting  $\text{Pb}^{2+}$  with a detection limit of 5 nM within 20 minutes <sup>75</sup>. Another similar turn-on fluorescent design was reported by the Liu group. In this design, the GR-5 DNAzyme catalyzed the reaction in *cis* (i.e., the cleavage reaction occurred intramolecularly) in order to bring the fluorophore in even closer contact with the AuNPs (Figure 1.11b) <sup>76</sup>. Furthermore, Wang and colleagues developed a sensitive fluorescent design that used gold nanorod as a fluorescence quencher and an 8-17 DNAzyme. Their results showed that their design was capable of highly sensitive  $\text{Pb}^{2+}$  detection, with a detection limit of 61.8 pM (Figure 1.11c) <sup>77</sup>.

Graphene oxide (GO) and carbon nanotubes (CNTs) are two nanomaterials that have been described as fluorescence super-quenchers. These sensing platforms have gained more recognition in recent years, mainly due to the fact that the ssDNA and dsDNA duplex exhibits different affinities toward GO and CNTs <sup>78,79</sup>. Both GO and CNTs have  $\pi$ -rich conjugation domains and can adsorb single-stranded DNA molecules via  $\pi$ - $\pi$  stacking interactions <sup>80</sup>. However, the more rigid double-stranded DNA with exposed negative charges has a limited affinity for CNTs and GOs, <sup>81</sup> and several studies have taken advantage of this property to develop “turn-off” fluorescence sensors (Figure 1.11 d). Under this approach, the DNAzyme and



substrate strands are hybridized before the targeted is added, and this duplex structure allows the strands to remain free in the solution. After the target is added, the substrate is cleaved and releases from the DNAzyme. The cleaved fluorescent single-stranded DNA can then be captured by the CNTs or GOs, thus quenching the fluorescence signal. This design was used with the 8-17 DNAzyme to detect  $Pb^{2+}$  with a detection limit of 1 nM<sup>82</sup>. Conversely, a “turn-on” fluorescent sensor was developed by minimizing the length of the single-stranded DNA that is released after RNA cleavage<sup>83</sup>. For “turn-on” sensors, minimal binding between FAM-labeled DNA and GOs is enabled by reducing the cleaved fluorescent sequence to a length of 5 residues, and the whole probe is immobilized on the GO by introducing a large ssDNA loop into the DNAzyme strand. Before the target is added, the ssDNA loop keeps the fluorescent probe bound to the GO, while once the target has been added, the cleaved FAM-labeled DNA can depart from the GO, thus providing a fluorescence signal (Figure 1.11e).

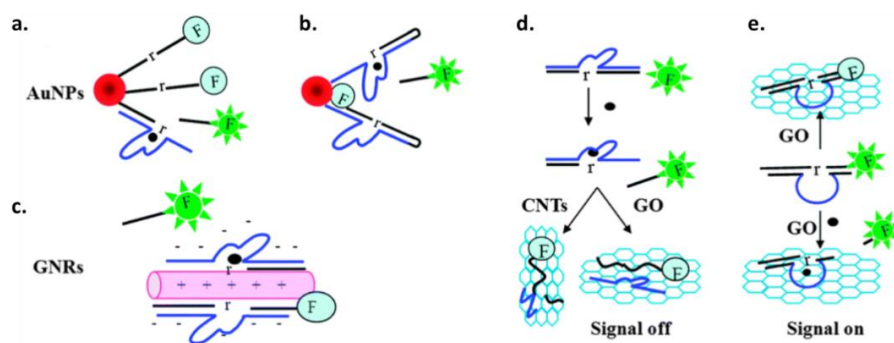


**Figure 1.11.** DNAzyme-based fluorescent biosensors. (a) DNA substrates with a fluorophore immobilized onto AuNPs for quenching. (b) A cis-conformation brings the fluorophore closer to the AuNP. (c) Many DNAzymes-substrate probes could be adsorbed onto gold nanorods for close contact quenching of the fluorophore. (d) Double-stranded DNA has limited affinity for graphene oxide and carbon nanotubes. Upon cleavage, the single-stranded fluorescent piece will be adsorbed onto these nanomaterials and become quenched. (e) A large ssDNA loop is introduced to keep the fluorescent probe bound to graphene oxide. Adjusting the length of the cleaved fluorescent strand allows it to depart from the graphene oxide, thus providing a fluorescent signal (adapted from Ref. <sup>84</sup>).

#### **1.4. Immobilization of biomolecules on sensing interfaces**

This section begins by introducing and reviewing the different strategies for immobilizing biomolecules before proceeding to a discussion of how the immobilization of DNAzymes onto different nanomaterials can be a useful approach to biosensor development.

##### **1.4.1. An overview of biomolecules immobilization**

Biomolecule immobilization appears as a key factor in developing efficient, high-performance biosensors that feature good operational and storage stability, high sensitivity, high selectivity, short response times, and high reproducibility. Immobilized biomolecule probes must be able to maintain their structure, maintain their function, retain their biological activity after immobilization, remain tightly bound to the surface, and not be desorbed during use. Moreover, an ideal biosensor must be stable in order to enable long-term use.

The immobilization of DNA molecules to a solid support has many potentially beneficial biotechnology- and molecular-biology-related applications, including environmental monitoring, food and quality control, and clinical analysis<sup>85-88</sup>. Numerous solid supports have been explored for DNA immobilization, including glass, ceramics, silicon wafers, magnetic beads, nylon, polymers, and membranes<sup>89-94</sup>. Similarly, many different strategies for immobilizing nucleic acids onto surfaces have also been explored, including entrapment, adsorption, cross-linking, covalent coupling, and affinity<sup>95</sup>. The selected immobilization method can have different effects on a biosensor's activity and stability. In addition, factors such as measurement accuracy, sensor-to-sensor reproducibility, and operational lifetime are drastically influenced by probe stability. Given the degree to which a biosensor's analytical performance is affected by the immobilization

process, it is unsurprising that researchers have been focusing their efforts on developing immobilization strategies that will assure maximum sensitivity and stability.

Each of the above-noted immobilization methods has advantages and drawbacks. As such, selecting the most appropriate technique will depend on the nature of the biomolecule probe, its transducer, and the associated detection mode. In addition, selecting the optimal immobilization method also depends on whether the biosensor application requires maximum sensitivity or maximum stability. Furthermore, it is also important to consider factors like reproducibility, cost, and the difficulty of the immobilization process. Sensitivity will decrease if the immobilization process causes probe denaturation or conformational changes, or if the probe has been modified, especially on its active site. Higher sensitivity can be obtained by using oriented immobilization to fix the biomolecule probes to the surface, or by selecting the spacer arm between the probe and the surface. Properly oriented probes correctly expose their active site to the solution phase, which results in better biosensor performance. Numerous immobilization techniques result in random distribution or poorly oriented probes. These outcomes can lead to partial or total activity loss due to probe denaturation, or they may result in the active site becoming blocked off from the target. Techniques based on the formation of affinity bonds between a functional group (e.g. (strept)avidin) on a support and an affinity tag (e.g. biotin) on a biomolecule sequence allow for biomolecule immobilization to occur in an ordered and site-specific manner, which in turn enables the development of efficient biosensors<sup>96</sup>. Moreover, the strong affinity between biotin and (strept)avidin—with a dissociation constant,  $K_d$  in the order of  $4 \times 10^{-14}$  M<sup>97</sup>—decreases the non-specific background due to the desorption or

displacement of probes by unintended targets. Like affinity interaction, self-assembled monolayer-based immobilization reduces the number of random orientations and generates uniform, reproducible, and stable structures with high levels of coverage <sup>96</sup>. Choosing the appropriate immobilization strategy is essential for avoiding the desorption of biomolecules from the surface, which can occur due to inadequate stability caused by different environmental conditions, such as ionic strength, pH, humidity, and temperature. In such cases, the issue of high background noise arises due to the nonspecific adsorption of oligonucleotides to the solid support.

#### **1.4.2. DNAzyme-nanomaterial based biosensors**

The use of nanomaterials (e.g. conducting polymer nanowires, carbon nanotubes, nanoparticles) in biosensing devices is an exciting and recent attempt to improve the performance of these detection platforms. Nanomaterials are extremely promising for such applications due to their unique properties. For example, carbon nanotubes have remarkable electrical, mechanical, and structural properties that can enhance the electrochemical reactivity of biomolecules <sup>98</sup>. Nanoparticles of different compositions and sizes have also been used in recent years as versatile and sensitive tracers for the electronic, optical, or microgravimetric transduction of different biomolecular recognition events <sup>99</sup>. In addition, metal nanoparticles feature excellent conductivity, which enables enhanced electron transfer between the biomolecule's redox center and the electrode surface <sup>100</sup>. Nanoparticles are interesting immobilization surfaces due to their large surface area <sup>100</sup>. Moreover, the direct adsorption of probes onto bulk metal surfaces frequently results in probe denaturation and bioactivity loss;

however, this can be avoided if the probes are first adsorbed onto the metal nanoparticles before being electrodeposited onto the electrode surface <sup>101</sup>. SiO<sub>2</sub> nanoparticles are also excellent matrices for probe immobilization due to their good biocompatibility and easy preparation <sup>100</sup>.

Combining DNazymes with nanomaterials not only allows the DNzyme's catalytic property to be retained, but it also introduces the nanomaterial's signal transformation function, thus achieving the integration of the identifying and signal transforming functions. This is particularly helpful for designing biosensors with high sensitivity, high selectivity, and high efficiency. Given these advantages, DNazymes have been widely combined with nanomaterials, such as graphene, gold nanoparticles, quantum dots, and magnetic nanomaterials in order to develop new biosensors. Some examples of DNzyme-based biosensors that incorporate nanomaterials such as gold nanoparticles, gold nanorods, graphene oxides, and carbon nanotubes were provided in Figure 1.11. Conversely, Figure 1.12 illustrates a DNzyme-based biosensor that uses magnetic nanomaterials to achieve sensitive and selective Pb<sup>2+</sup> detection <sup>102</sup>. As can be seen, the GR-5 DNzyme has been labeled with a fluorophore (F) as the fluorescence reporter at the 5' end, and a biotin for the conjugation with the streptavidin-coated magnetic bead at the 3' end. Upon the addition of Pb<sup>2+</sup>, the double-quencher-labeled substrate strand is cleaved and disassociated from the GR-5 DNzyme, recovering the fluorescence signal of the fluorophore. The use of magnetic nanomaterials as separation elements effectively reduced the background signal and allowed for highly sensitive detection. Moreover, the use of magnetic nanoparticles can also reduce the interference from real samples.

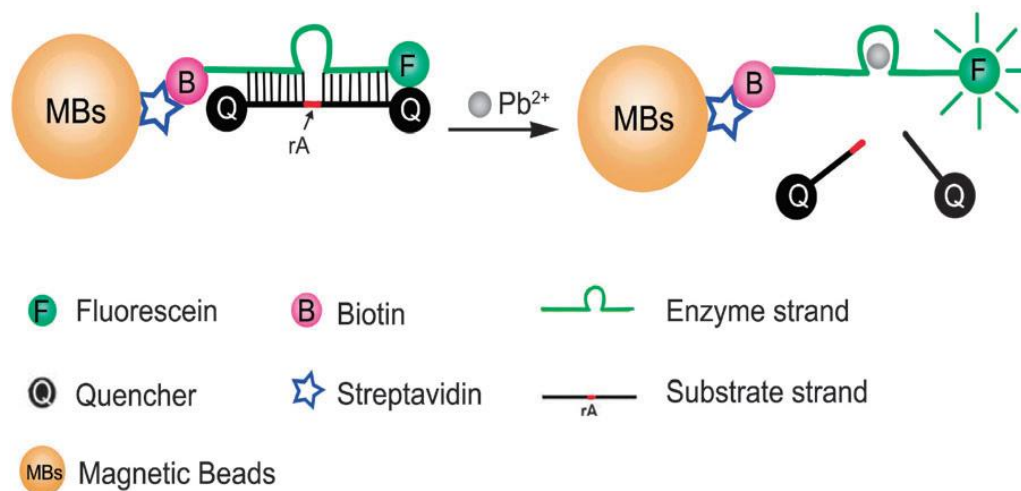


**Figure 1.12.** Schematic illustration of the DNAzyme-magnetic-bead-based biosensor (adapted from Ref. <sup>102</sup>).

It is well-known that selecting the appropriate material for DNAzyme immobilization requires an in-depth understanding of the physical and chemical interactions involved <sup>103</sup>. Therefore, these interactions must be investigated in further depth in order to identify the optimal material for DNAzyme immobilization, as well as the best immobilization strategy for developing stable DNAzyme-based biosensors.

### 1.5. Objective and thesis outline

Pathogenic bacteria pose a serious threat to public health, accounting for thousands of infections and deaths around the world each year. As such, the early and accurate detection of such bacteria is of the utmost importance in efforts to combat the resultant infections and diseases. Although many current detection strategies are hampered by various technical and cost limitations, DNA-based biosensors may be one technology with the potential to overcome these shortcomings. Thus, the overall objective of this work is to develop a DNAzyme-based biosensor

for the detection of pathogenic bacteria. More specifically, this research aims to develop a simple bead-based assay for the detection of *Escherichia coli* (*E. coli*) that uses an RNA-cleaving DNAzyme as its molecular recognition element. This bead-based assay will enable the sensitive detection of *E. coli* in both water samples and complex sample matrices, such as milk and apple juice, through the generation of a fluorescence signal. Furthermore, this method is capable of successfully decreasing the non-specific background signal through the implementation of a simple partitioning step. This is a critical requirement for the development of biosensors with lower limits of detection that is simply not possible in solution-based assays. Moreover, our simple-to-perform assay eliminates the need for specialized equipment and trained personnel by combining the advantages of agarose beads, which are cheap and widely available, and an easy-to-implement filtration step.

More detailed, objectives are the following:

- ❖ To examine three different materials for *E. coli*-specific DNAzyme immobilization: reduced graphene oxide, magnetic beads, and agarose beads.
- ❖ To compare *E. coli*-specific DNAzyme behavior in immobilized DNAzyme on agarose beads and DNAzyme in solution. These assessments include comparisons of following in bead-based and solution-based assays: kinetic analysis of the DNAzyme's activity, DNAzyme's sensitivity and specificity, and truncation analysis of the DNAzyme. Specifically, two DNAzyme constructs, full-length DNAzyme (Full DNAzyme) and its truncated sequence, (Short DNAzyme) are studied.

Master's Thesis - Sahar Esmaeili Samani  
McMaster University – Department of Chemical Engineering

- ❖ To demonstrate the bead-based biosensor's performance in detecting *E. coli* in water samples and complex matrices, such as milk and apple juice.



## 1.6. References

1. Tallury, P., Malhotra, A., Byrne, L. M. & Santra, S. Nanobioimaging and sensing of infectious diseases. *Adv. Drug Deliv. Rev.* **62**, 424–437 (2010).
2. Kaittanis, C., Santra, S. & Perez, J. M. Emerging nanotechnology-based strategies for the identification of microbial pathogenesis. *Adv. Drug Deliv. Rev.* **62**, 408–423 (2010).
3. Lazcka, O., Del, F. J. & Mu, F. X. Pathogen detection: A perspective of traditional methods and biosensors. **22**, 1205–1217 (2007).
4. Skottrup, P. D., Nicolaisen, M. & Justesen, A. F. Towards on-site pathogen detection using antibody-based sensors. *Biosens. Bioelectron.* **24**, 339–348 (2008).
5. Mao, X. *et al.* Disposable nucleic acid biosensors based on gold nanoparticle probes and lateral flow strip. *Anal. Chem.* **81**, 1660–1668 (2009).
6. Leonard, P. *et al.* Advances in biosensors for detection of pathogens in food and water. *Enzyme Microb. Technol.* **32**, 3–13 (2003).
7. Black, E. K. & Finch, G. R. Detection and Occurrence of Waterborne Bacterial and Viral Pathogens. *Source Water Environ. Res. Lit. Rev.* **66**, 292–298 (1994).
8. Atlas, R. M. Legionella: From environmental habitats to disease pathology, detection and control. *Environ. Microbiol.* **1**, 283–293 (1999).
9. Khabbaz, R. F., Moseley, R. R., Steiner, R. J., Levitt, A. M. & Bell, B. P. Challenges of infectious diseases in the USA. *Lancet* **384**, 53–63 (2014).
10. Curtis, D., Hill, A., Wilcock, A. & Charlebois, S. Foodborne and waterborne pathogenic bacteria in selected Organisation for Economic Cooperation and Development (OECD) Countries. *J. Food Sci.* **79**, R1871–R1876 (2014).
11. Vouga, M. & Greub, G. Emerging bacterial pathogens: The past and beyond. *Clin. Microbiol. Infect.* **22**, 12–21 (2016).
12. Hamula, C. L. A. *et al.* Selection and analytical applications of aptamers binding microbial pathogens. *TrAC - Trends Anal. Chem.* **30**, 1587–1597 (2011).
13. Li, F. *et al.* Detection of escherichia coli O157:H7 using gold nanoparticle labeling and inductively coupled plasma mass spectrometry. *Anal. Chem.* **82**, 3399–3403 (2010).
14. Velusamy, V., Arshak, K., Korostynska, O., Oliwa, K. & Adley, C. An overview of foodborne pathogen detection: In the perspective of biosensors. *Biotechnol. Adv.* **28**, 232–

- 254 (2010).
15. Peters, R. P. H., Agtmael, M. A. Van, Danner, S. A., Savelkoul, P. H. M. & Vandenbroucke-Grauls, C. M. J. E. New developments in the diagnosis of bloodstream infections. *Lancet Infect. Dis.* **4**, 751–760 (2004).
  16. Ahmed, A., Rushworth, J. V., Hirst, N. A. & Millner, P. A. Biosensors for whole-cell bacterial detection. *Clin. Microbiol. Rev.* **27**, 631–646 (2014).
  17. Chames, P., Van Regenmortel, M.; Weiss, E.; Baty, D. Therapeutic antibodies: Successes, limitations and hopes for the future. *Br. J. Pharmacol.* **157**, 220–233 (2009).
  18. Yaron, S. & Matthews, K. R. A reverse transcriptase-polymerase chain reaction assay for detection of viable *Escherichia coli* O157:H7: Investigation of specific target genes. *J. Appl. Microbiol.* **92**, 633–640 (2002).
  19. World Health Organization (WHO). Millennium Development Goals: Progress towards the Health-Related Millennium Development Goals. Available at: [http://www.who.int/topics/millennium\\_development\\_goals/en/](http://www.who.int/topics/millennium_development_goals/en/). (Accessed: 17th February 2015)
  20. Luong, J. H. T., Male, K. B. & Glennon, J. D. Biosensor technology : Technology push versus market pull. **26**, 492–500 (2008).
  21. Alberts, B., Alexander, J., Lewis, J., Raff, M., Roberts, K., Walter, P. *Molecular Biology of the Cell.* (2004).
  22. Liu, J., Cao, Z. & Lu, Y. *Functional Nucleic Acid Sensors.* **109**, (2009).
  23. Breaker, R. R. & Joyce, G. F. A DNA enzyme that cleaves RNA. *Chem. Biol.* **1**, 223–229 (1994).
  24. Jijakli, K. *et al.* The in vitro selection world. *Methods* **106**, 3–13 (2016).
  25. Tuerk, C., Gold, L. Systematic Evolution of Ligands by Exponential Enrichment : RNA Ligands to Bacteriophage T4 DNA Polymerase. **249**, 505–510 (2018).
  26. Gysbers, R.; Tram, K.T.; Manochery, S.; Chang, D.; Li, Y. *Selection and application of catalytically active oligonucleotides.* (Pan Stanford: Boca Raton, FL, USA, 2016).
  27. Reaker, R. O. R. B. Cleaving DNA with DNA. **95**, 2233–2237 (1998).
  28. Sreedhara, A., Li, Y. & Breaker, R. R. Ligating DNA with DNA. 3454–3460 (2004). doi:10.1021/ja039713i

29. Reaker, R. O. R. B. Phosphorylating DNA with DNA. **96**, 2746–2751 (1999).
30. Sheppard, T. L., Ordoukhanian, P. & Joyce, G. F. A DNA enzyme with N-glycosylase activity. **2000**, (2000).
31. Li, Y., Sen, D. A catalytic DNA for Porphyrin Metallation. *Nat. Struct. Mol. Biol.* **3**, 743 (1996).
32. Kruger, K.; Grabowski, P. J.; Zaug, A. J.; Sands, J.; Gottschling, D. E.; Cech, T. R. Self-splicing RNA: autoexcision and autocyclization of the ribosomal RNA intervening sequence of Tetrahymena. *Cell* **31**, 147–157 (1982).
33. Santoro, S. W. & Joyce, G. F. A general purpose RNA-cleaving DNA enzyme. *Proc. Natl. Acad. Sci.* **94**, 4262–4266 (1997).
34. Faulhammer, D., Famulok, M. The Ca<sup>2+</sup> Ion as a Cofactor for a Novel RNA-Cleaving Deoxyribozyme. *Angew. Chemie Int. Ed. English* **35**, 2837–2841 (1996).
35. Li, J., Zheng, W., Kwon, A. H. & Lu, Y. In vitro selection and characterization of a highly efficient Zn(II)-dependent RNA-cleaving deoxyribozyme. *Nucleic Acids Res.* **28**, 481–488 (2000).
36. Cruz, R. P.; Withers, J. B.; Li, Y. Dinucleotide Junction Cleavage Versatility of 8-17 Deoxyribozyme. *Chem. Biol.* **11**, 57–67 (2004).
37. Grunert, H. *et al.* RNA cleaving '10-23' DNAzymes with enhanced stability and activity. **31**, 5982–5992 (2003).
38. Wang, D. Y. & Sen, D. A Novel Mode of Regulation of an RNA-cleaving DNAzyme by Effectors that Bind to Both Enzyme and Substrate. (2001). doi:10.1006/jmbi.2001.4811
39. Ali, M. M., Aguirre, S. D., Lazim, H. & Li, Y. Fluorogenic DNAzyme probes as bacterial indicators. *Angew. Chemie - Int. Ed.* **50**, 3751–3754 (2011).
40. Zhang, W., Feng, Q., Chang, D., Tram, K. & Li, Y. In vitro selection of RNA-cleaving DNAzymes for bacterial detection. *Methods* **106**, 66–75 (2016).
41. Silverman, S. K. Catalytic DNA (deoxyribozymes) for synthetic applications-current abilities and future prospects. *Chem. Commun.* 3467–3485 (2008). doi:10.1039/b807292m
42. DeRose, V. J. Metal ion binding to catalytic RNA molecules. *Curr. Opin. Struct. Biol.* **13**, 317–324 (2003).
43. Santoro, S. W. & Joyce, G. F. Mechanism and utility of an RNA-cleaving DNA enzyme.

- Biochemistry* **37**, 13330–13342 (1998).
44. Ward, W. L., Plakos, K. & Derose, V. J. Nucleic acid catalysis: Metals, nucleobases, and other cofactors. *Chem. Rev.* **114**, 4318–4342 (2014).
  45. Takagi, Y. SURVEY AND SUMMARY: Recent advances in the elucidation of the mechanisms of action of ribozymes. *Nucleic Acids Res.* **29**, 1815–1834 (2001).
  46. Wirmer-Bartoschek, J. & Schwalbe, H. Understanding How DNA Enzymes Work. *Angew. Chemie - Int. Ed.* **55**, 5376–5377 (2016).
  47. Turner, A.; Karube, I.; Wilson, G. . *Biosensors: Fundamentals and Applications*. (Oxford University Press, 1987).
  48. Clark, L.C., Jr.; Lyons, C. Electrode systems for continuous monitoring in cardiovascular surgery. *Ann. N. Y. Acad. Sci.* **102**, 29–45 (1962).
  49. Guilbault, G.G. and Montalvo, Jr, J. . Urea-specific enzyme electrode. *J. Am. Chem. Soc.* **91**, 2164–2165 (1969).
  50. Wang, J. Glucose Biosensors : 40 Years of Advances and Challenges. 983–988 (2001).
  51. P.F. Turner, A. Biosensors: sense and sensibility. *Chem Soc Rev* **42**, 3184–3196. (2013).
  52. Bousse, L. Whole cell biosensors. *Sens. Actuators B Chem.* **34**, 270–275 (1996).
  53. Wang, J. Electrochemical nucleic acid biosensors. *Anal. Chim. Acta.* **469**, 63–71 (2002).
  54. Campàs, M., Carpentier, R. & Rouillon, R. Plant tissue-and photosynthesis-based biosensors. **26**, 370–378 (2008).
  55. Bang, G. S., Cho, S. & Kim, B. A novel electrochemical detection method for aptamer biosensors. **21**, 863–870 (2005).
  56. Wang, J., Jiang, Y., Zhou, C. & Fang, X. Aptamer-Based ATP Assay Using a Luminescent Light Switching Complex. **77**, 3542–3546 (2005).
  57. Stojanovic, M. N., Prada, P. De & Landry, D. W. Aptamer-Based Folding Fluorescent Sensor for Cocaine. **4**, 4928–4931 (2001).
  58. Stojanovic, M. N. & Landry, D. W. Aptamer-Based Colorimetric Probe for Cocaine. 9678–9679 (2002). doi:10.1021/ja0259483
  59. Aguirre, S. D., Ali, M. M., Salena, B. J. & Li, Y. A sensitive DNA enzyme-based

- fluorescent assay for bacterial detection. *Biomolecules* **3**, 563–577 (2013).
60. Tram, K., Kanda, P. & Li, Y. Lighting Up RNA-cleaving DNazymes for biosensing. *J. Nucleic Acids* **2012**, (2012).
  61. Gong, L. *et al.* DNzyme-based biosensors and nanodevices. 979–995 (2015). doi:10.1039/c4cc06855f
  62. Navani, N. K. & Li, Y. Nucleic acid aptamers and enzymes as sensors. *Curr. Opin. Chem. Biol.* **10**, 272–281 (2006).
  63. Chem, A. *et al.* Real-Time Characterization of Ribozymes by Fluorescence Resonance Energy Transfer. **19**, 1997–2000 (1999).
  64. Stojanovic, M. N., Prada, P. De & Landry, D. W. Homogeneous assays based on deoxyribozyme catalysis. **28**, 2915–2918 (2000).
  65. Perkins, T. A. *et al.* Fluorescence Resonance Energy Transfer Analysis of Ribozyme Kinetics Reveals the Mode of Action of a Facilitator Oligonucleotide. **2960**, 16370–16377 (1996).
  66. Lu, Y. *et al.* New highly sensitive and selective catalytic DNA biosensors for metal ions. **18**, (2003).
  67. Liu, J. & Lu, Y. Improving Fluorescent DNzyme Biosensors by Combining Inter- and Intramolecular Quenchers. **75**, 6666–6672 (2003).
  68. Liu J, Brown AK, Meng X, Cropek DM, Istok JD, et al. A catalytic beacon sensor for uranium with parts-per-trillion sensitivity and millionfold selectivity. *Proc Natl Acad Sci USA*. **104**, 2056–2061 (2007).
  69. Mei, S. H. J., Liu, Z., Brennan, J. D. & Li, Y. An Efficient RNA-Cleaving DNA Enzyme that Synchronizes Catalysis with Fluorescence Signaling. 3106–3114 (2003). doi:10.1021/ja0281232
  70. Chiuman, W. & Li, Y. Evolution of High-Branching Deoxyribozymes from a Catalytic DNA with a Three-Way Junction. 1061–1069 (2006). doi:10.1016/j.chembiol.2006.08.009
  71. Chiuman, W. & Li, Y. Efficient signaling platforms built from a small catalytic DNA and doubly labeled fluorogenic substrates. **35**, 401–405 (2007).
  72. Kandadai, S. A., Mok, W. W. K., Ali, M. M. & Li, Y. Characterization of an RNA-cleaving deoxyribozyme with optimal activity at pH 5. *Biochemistry* **48**, 7383–7391 (2009).

73. Shen, Y. *et al.* Entrapment of Fluorescence Signaling DNA Enzymes in Sol - Gel-Derived Materials for Metal Ion Sensing. **79**, 3494–3503 (2007).
74. Liu, Z., Mei, S. H. J., Brennan, J. D. & Li, Y. Assemblage of Signaling DNA Enzymes with Intriguing Metal-Ion Specificities and pH Dependences. 7539–7545 (2003).
75. Kim, J. H., Han, S. H. & Chung, B. H. Biosensors and Bioelectronics Improving Pb<sup>2+</sup> detection using DNAzyme-based fluorescence sensors by pairing fluorescence donors with gold nanoparticles. *Biosens. Bioelectron.* **26**, 2125–2129 (2011).
76. Online, V. A. *et al.* A highly sensitive and selective biosensing strategy for the detection of Pb<sup>2+</sup> ions based on GR-5 DNAzyme functionalized AuNPs. 2557–2563 (2013). doi:10.1039/c3nj00328k
77. Wang, L., Jin, Y., Deng, J. & Chen, G. Gold nanorods-based FRET assay for sensitive detection of Pb<sup>2+</sup> using 8-17DNAzyme. 5169–5174 (2011). doi:10.1039/c1an15783c
78. Yang, R. *et al.* Carbon Nanotube-Quenched Fluorescent Oligonucleotides : Probes that Fluoresce upon Hybridization. 8351–8358 (2008).
79. Lu, C., Yang, H., Zhu, C., Chen, X. & Chen, G. A Graphene Platform for Sensing Biomolecules. *Angew Chem.* **48**, 4879–4881 (2009).
80. Varghese, N. *et al.* Binding of DNA nucleobases and nucleosides with graphene. *ChemPhysChem* **10**, 206–210 (2009).
81. Zheng, M. *et al.* DNA-assisted dispersion and separation of carbon nanotubes. *Nat Mater* **2**, 338–342 (2003).
82. Links, D. A. Combing DNAzyme with single-walled carbon nanotubes for detection of Pb<sup>2+</sup>. 764–768 (2011). doi:10.1039/c0an00709a
83. Zhao, X. *et al.* Graphen-DNAzyme Based Biosensor for Amplified Fluorescence “Turn-On” Detection of Pb<sup>2+</sup> with a high selectivity. *Anal Chem.* **83**, 5062–5066 (2011). doi:10.1021/ac200843x
84. Gong, L. *et al.* DNAzyme-based biosensors and nanodevices. *Chem. Commun.* **51**, 979–995 (2015).
85. Yousefi, H., Ali, M. M., Su, H. M., Filipe, C. D. M. & Didar, T. F. Sentinel Wraps: Real-Time Monitoring of Food Contamination by Printing DNAzyme Probes on Food Packaging. *ACS Nano* **12**, 3287–3294 (2018).
86. Malhotra, B. D. & Chaubey, A. Biosensors for clinical diagnostics industry. *Sensors*

- Actuators, B Chem.* **91**, 117–127 (2003).
87. Andreescu, S. & Marty, J. L. Twenty years research in cholinesterase biosensors: From basic research to practical applications. *Biomol. Eng.* **23**, 1–15 (2006).
  88. Mello, L. D. & Kubota, L. T. Review of the use of biosensors as analytical tools in the food and drink industries. *Food Chem.* **77**, 237–256 (2002).
  89. Joos, B., Kuster, H. & Cone, R. Covalent attachment of hybridizable oligonucleotides to glass supports. *Anal. Biochem.* **247**, 96–101 (1997).
  90. Chrisey, L. Covalent attachment of synthetic DNA to self-assembled monolayer films. *Nucleic Acids Res.* **24**, 3031–3039 (1996).
  91. John, M., Hughes, G. & Andrews, D. W. Preparation of Magnetic Oligo(dT) Particles. **20**, 2–3 (1996).
  92. Lamture, J. B. *et al.* Direct detection of nucleic acid hybridization on the surface of a charge coupled device. **22**, 2121–2125 (1994).
  93. Piunno, P. A. E., Krull, U. J., Hudson, R. H. E., Damha, M. J. & Cohen, H. Fiber optic biosensor for fluorimetric detection of DNA hybridization. *Anal. Chim. Acta* **288**, 205–214 (1994).
  94. Cohen G, Deutsch J, Fineberg J, L. A. Covalent attachment of DNA oligonucleotides to glass. *Nucleic Acids Res* **25**, 911–912 (1997).
  95. Sassolas, A., Blum, L. J. & Leca-Bouvier, B. D. Immobilization strategies to develop enzymatic biosensors. *Biotechnol. Adv.* **30**, 489–511 (2012).
  96. Campas, M., Bucur, B., Andreescu, S. & Marty, J. L. Application of oriented immobilization to enzyme sensors. *Curr. Top. Biotechnol.* **1**, 95–107 (2004).
  97. Holmberg, A. *et al.* The biotin-streptavidin interaction can be reversibly broken using water at elevated temperatures. *Electrophoresis* **26**, 501–510 (2005).
  98. Wang, J. Carbon-Nanotube Based Electrochemical Biosensors : A Review. 7–14 (2005). doi:10.1002/elan.200403113
  99. Wang, J. reviews Nanomaterial-Based Amplified Transduction of Biomolecular Interactions. 1036–1043 (2005). doi:10.1002/sml.200500214
  100. Luo, X., Morrin, A., Killard, A. J. & Smyth, M. R. Application of nanoparticles in electrochemical sensors and biosensors. *Electroanalysis* **18**, 319–326 (2006).

101. Liu, G., Lin, Y., Ostatna, V. & Wang, J. Enzyme nanoparticles-based electronic biosensor. 3481–3483 (2005). doi:10.1039/b504943a
102. Nie, D. *et al.* A sensitive and selective DNAzyme-based flow cytometric method for detecting Pb<sup>2+</sup> ions. *Chem. Commun.* **48**, 1150–1152 (2012).
103. Gibbs, J., Kennebunk, M. Immobilization Principles – Selecting the Surface. *ELISA Technical Bulletin*. **1**, 1-8 (2001).



## **2. Development of a bead-based assay for the detection of *E.coli* using DNAzymes**

Sahar Esmacili Samani<sup>1,2</sup>, Erin M. McConnell<sup>2</sup>, Dingran Chang<sup>2</sup>, Carlos D.M. Filipe<sup>1</sup> and  
Yingfu Li<sup>2</sup>

*1. Department of Chemical Engineering, McMaster University, 1280 Main St. W., Hamilton, ON  
L8S 4L7, Canada.*

*2. Department of Biochemistry and Biomedical Sciences, McMaster University, 1280 Main St.  
W., Hamilton, ON L8S 4K1, Canada.*

## 2.1. Abstract

This chapter reports on a simple, easy-to-use, and low-cost bead-based assay for *E. coli* detection. The proposed method utilizes a bacteria-specific RNA-cleaving DNase probe, which generates a fluorescence signal in the presence of a target bacterium. This fluorescence signal can then be interpreted by a non-expert using a simple hand-held fluorescence device. When coupled with a simple filtration step, the immobilization of the biotinylated DNase onto the surface of streptavidin-coated agarose beads enabled the sensitive detection of *E. coli* in both water samples and complex sample matrices, such as milk and apple juice. In addition, this work also presents a comparison of solution-based and bead-based assays for detecting *E. coli* via an *E. coli*-specific DNase. The bead-based assay presented here can produce a strong fluorescence signal readout in as little as 2.5 min following contact with *E. coli*, and it is capable of achieving a detection limit of 1,000 colony-forming units (CFUs) without sample enrichment. Our results demonstrate that the bacterial-detection assay described in this work is highly attractive for field applications, especially in resource-limited regions.

**Keywords:** RNA-cleaving DNase, immobilization, agarose beads, biosensors, bacterial detection, fluorescence assay

## 2.2. Introduction

The development of sensors that are reliable, sensitive, cost-effective, and portable is critical to the creation of biological assays and point-of-care (POC) diagnostics. Solution-based assays are not necessarily optimal for use in POC diagnostics and field applications, especially in resource-limited regions; indeed, solid-phase assays can significantly simplify experimental procedures, thus making them well suited for biosensor development. Moreover, solid-phase sensors offer a number of important advantages not afforded by solution-based assays, such as excellent stability, the potential for sensor regeneration, and long-term storage<sup>1-7</sup>. In addition, solid-phase assays also feature the advantage of reduced background signal generation, which is a principal limitation when working at low target concentrations and is the key driving force behind efforts to produce sensors with ever lower limits of detection<sup>3,4,7-9</sup>.

The immobilization of DNAzymes to a solid support has many biotechnology and molecular biology applications, including environmental monitoring, food and quality control, and clinical analyses<sup>6,10-12</sup>. Catalytic DNA molecules (DNAzymes or Deoxyribozymes) are chemically synthesized single-stranded DNA molecules that exhibit high chemical stability, as well as excellent recognition specificity and affinity for their targets. Moreover, DNAzymes can be easily chemically modified to introduce functional groups, which in turn allows for simple conjugation chemistry. This strategy has been commonly used to facilitate the linking of DNAzymes to various nanomaterials<sup>13</sup>. Due to these advantages, DNAzymes have come to be regarded as excellent recognition elements for use in biosensor development<sup>14-22</sup>. In RNA-cleaving DNAzymes, the target binding event is linked to the cleavage of an RNA-containing

substrate <sup>17,22–24</sup>. Furthermore, these RNA-cleaving DNazymes can be integrated with various signal transduction mechanisms to produce fluorescent, colorimetric, electrochemical, and chemiluminescent biosensing <sup>10,25–31</sup>.

In biosensor development, the required interactions of the system can be simplified by immobilizing one component. To this end, researchers have explored various solid supports for immobilizing DNA, including glass, magnetic beads, ceramics, silicon wafer, nylon, polymers, and membranes <sup>32–37</sup>. Immobilization can be achieved through a variety of mechanisms, such as entrapment, adsorption, cross-linking, covalent coupling, and affinity <sup>3</sup>. The judicious selection of an immobilization strategy is essential for avoiding the desorption of biomolecules from the surface, which can occur due to inadequate stability under different environmental conditions, such as ionic strength, pH, humidity, and temperature. In such cases, the issue of high background noise emerges as a result of the nonspecific adsorption of oligonucleotides to the solid support.

Nanomaterials that have been functionalized with DNA are a promising option for the development of stable and portable biosensors <sup>13</sup>. In this work, we examined three different materials for *E. coli*-specific DNzyme immobilization: reduced graphene oxide, magnetic beads, and agarose beads. The agarose beads produced the highest signal-to-background ratio and, as such, were chosen for DNzyme immobilization. We then conducted a comprehensive study comparing *E. coli*-specific DNzyme behavior in immobilized DNzyme on agarose beads and DNzyme in solution. Specifically, two DNzyme constructs, full-length DNzyme (Full DNzyme) and its truncated sequence (Short DNzyme) were studied. As the results of

this investigation show, the coupling of immobilized DNAzyme on agarose beads and filtration enabled the sensitive detection of *E. coli* in water samples and complex sample matrices, such as milk and apple juice. This bead-based assay was able to successfully decrease the non-specific background via a simple partitioning step, which is a critical requirement for developing biosensors with lower limits of detection that is simply not possible in solution-based assays.

## **2.3. Results and Discussion**

### **2.3.1. Kinetic analysis of the Full DNAzyme's activity in solution and immobilized on agarose beads**

Three different materials were examined for *E. coli*-specific DNAzyme immobilization: reduced graphene oxide, magnetic beads, and agarose beads. Reduced graphene oxide has  $\pi$ -rich conjugation domains and can adsorb single-stranded nucleic acid molecules, such as DNAzymes, via  $\pi$ - $\pi$  stacking interactions<sup>38</sup>. This non-covalent attachment allows the DNAzyme to be desorbed or displaced by unintended targets, which consequently produces high non-specific background signal. Since magnetic beads and agarose beads are coated with streptavidin, biotinylated DNAzyme can be immobilized onto these materials through the highly specific biotin-streptavidin interaction. The strong affinity between biotin and streptavidin, with a dissociation constant,  $K_d$ , in the order of  $4 \times 10^{-14}$  M<sup>39</sup>, decreases the non-specific background due to the desorption or displacement of the DNAzyme by unintended targets. Ultimately, agarose beads were selected for this research, as they produced the highest signal-to-background ratio (see Supplementary Information, Figure S1). Agarose beads were also larger than the magnetic beads (35  $\mu\text{m}$  comparing to 1.5  $\mu\text{m}$  for agarose beads and magnetic beads

respectively), which may further explain their superior performance, as more surface area means a greater number of binding sites for DNAszymes. Nonetheless, it is agarose beads' ability to produce a high signal-to-background ratio that makes them highly suitable for use in biosensor development.

Next, a kinetic analysis was performed to investigate whether immobilizing the DNAszyme onto the surface of the agarose beads affected its cleavage activity in the presence of *E. coli*. After attaching to the agarose beads, the DNAszyme's movement is relatively restricted compared to free DNAszyme in solution. Therefore, we hypothesized that this restriction may decrease the DNAszyme's response toward the target, as immobilization-induced restriction might make it less accessible to its target, especially with low amounts of *E. coli* cells.

To test this hypothesis, we conducted a time-point study to analyze the activity of the Full DNAszyme in both solution-based and bead-based assays. This study consisted of an incubation time of 0-120 min as specified in Figure 2.1 at room temperature with a high and low number of cells ( $10^6$  and  $10^4$  *E. coli* cells, respectively). The sequence of the DNAszyme is provided in Supplementary Information, Table S1. Each experiment was conducted in a final concentration of  $1\times$  reaction buffer ( $1\times$  RB; 50 mM HEPES, pH 7.5, 150 mM NaCl, 15 mM MgCl<sub>2</sub>), with the reaction mixtures being analyzed via 10% denaturing polyacrylamide gel electrophoresis (dPAGE), (See Methods section for details on calculation of percent cleavage). These results are illustrated in Figure 2.1.

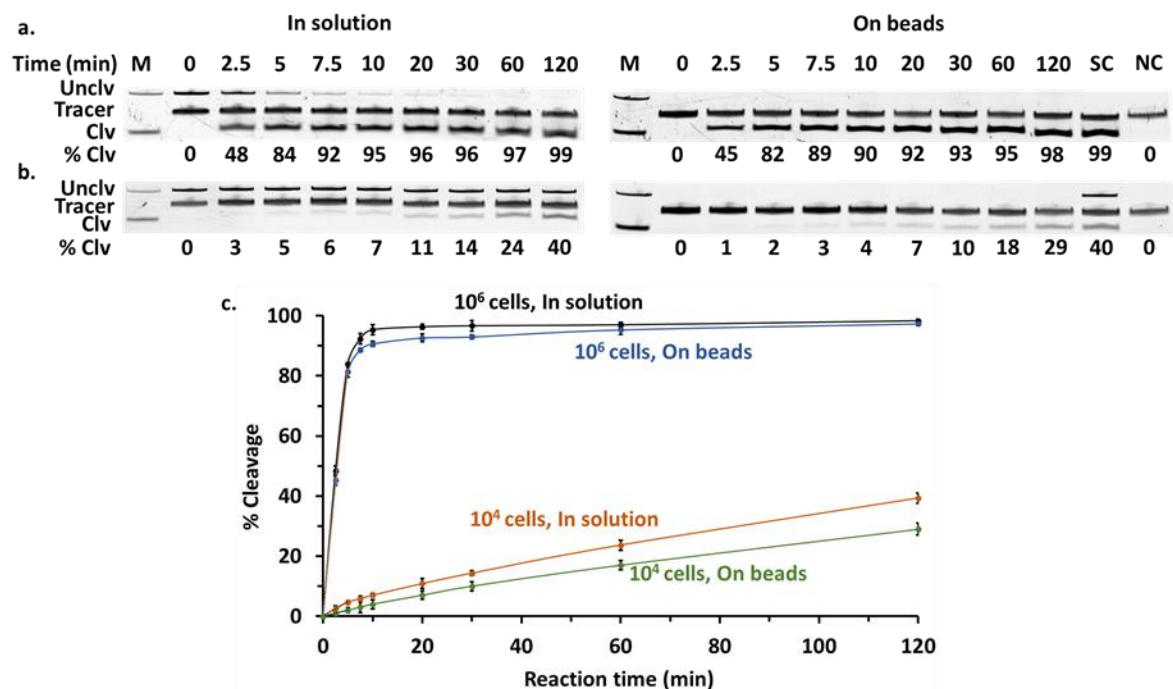


**Figure 2.1.** Kinetic analysis of Full DNazyme activity with (a)  $10^6$  *E. coli* cells and (b)  $10^4$  *E. coli* cells. The left part shows the solution-based assay and the right part shows the bead-based assay. 10% dPAGE analysis was performed for each reaction mixture, followed by fluorescence imaging with Typhoon and analysis with ImageQuant software. Cleavage product (Clv), full length DNazyme (which is uncleaved (Unclv)), and Tracer contain FAM and can be visualized via fluorescence scanning. The marker (M) is a sample of the DNazyme that has been heat treated with NaOH (at 90 °C for 5 min) in order to reveal the locations of the Clv and Unclv bands. The % Clv for each sample was calculated using the internal control, referred to as “Tracer” in the gel images (see Methods section for details). The lane of the bead-based samples, identified as “SC” in the gel images, is the Solution-Based Control (the last lane from the corresponding left part), which was added to confirm the accuracy of the calculations (see Methods section for details). NC represents the Negative Controls which are the samples that do not contain *E. coli*. (c) The bottom graph depicts the kinetic profiles associated with DNazyme activity for the solution- and bead-based assays. The data shown in this chart are the average of three independent experiments, and the error bars are based on the standard deviations of triplicate experiments.

As the results in Figure 2.1 show, ~90% cleavage was observed after 7.5 min and 10 min in the solution-based and bead-based assays, respectively, when a high number of *E. coli* cells were present ( $10^6$  cells). The initial cleavage percentage rates were obtained for both assays by fitting the linear region of the curves in Figure 2.1c, with values of 16.8 % Clv/min and 16.3% Clv/min being obtained for the solution-based and bead-based assays, respectively. As the black

and blue curves in Figure 2.1c illustrate, these results are comparable. For the tests using low numbers of *E. coli* cells ( $10^4$  cells), the DNAzyme's response was slower for the bead-based assay than it was during the solution-based assay: an initial cleavage rate of 0.9 %Clv/min for the solution-based assay, and a rate of 0.4 %Clv/min for the bead-based assay (comparing Orange and Green curves, Figure 2.1c). Interestingly, even with a low number of cells, both assays exhibited comparable behavior in that the DNAzyme's response toward its target could be increased by increasing incubation time.

When compared to the previously reported RNA-cleaving fluorogenic DNAzyme for *E. coli* (RFD-EC1) (see Supplementary Information, Figure S2 for details about how we modified our probe), our probe exhibited superior cleavage activity with both  $10^6$  and  $10^4$  *E. coli* cells. In previous solution-based work with RFD-EC1, 79% and 13% cleavage was observed with  $10^6$  and  $10^4$  *E. coli* cells, respectively, after a 1 hr incubation period at room temperature <sup>40</sup>. In contrast, our modified probe resulted in 97% and 24% cleavage with  $10^6$  and  $10^4$  *E. coli* cells, respectively, in the solution-based assay after a 1 hr reaction at room temperature. Furthermore, our probe showed faster response than the RFD-EC1 probe in the presence of the target with both  $10^6$  and  $10^4$  *E. coli* cells <sup>40</sup>. Considered together, these results show that immobilizing the DNAzyme on agarose beads maintains its cleavage activity, which in turn allows this solid support to be utilized in the development of an *E. coli*-detection biosensor.



### **2.3.2. Detection sensitivity of the Full DNAzyme in solution compared to immobilized on agarose beads**

Previously, researchers have reported methods capable of yielding limits of detection (LODs) between  $10^3$  - $10^5$  *E. coli* cells for *E. coli* DNAzyme incubated with *E. coli* cells for 1 hr<sup>26,40</sup>. However, these methods have either utilized solution-based assays or require relatively long incubation times and/or further manipulation, which is a drawback for developing a fast, on-site technology for detecting *E. coli*<sup>10,25,41</sup>. Thus, we were interested in evaluating the detection sensitivity of our DNAzyme, which was modified by changing the ligation site of the probe and eliminating the quencher from the substrate (see Supplementary Information, Figure S2 for details). In addition, detection sensitivity was also evaluated after the DNAzyme was immobilized onto a solid support in order to determine whether immobilization affected detection sensitivity. To this end, eight crude intracellular mixtures (CIMs) of *E. coli* were prepared from serially diluted *E. coli* samples, each of which contained a specific number of *E. coli* cells ranging from  $1 - 10^7$  (see the Methods section for details). The CIMs were tested with the Full DNAzyme using both bead-based and solution-based assays. Two reaction mixtures were prepared for each dilution: one that was incubated at room temperature for 1 hr, and one that was incubated at room temperature for 12 hrs. The purpose of this experiment was to determine whether better sensitivity could be achieved by increasing the amount of time the DNAzyme was incubated with the CIM. After each reaction mixture had been incubated, a 10% dPAGE analysis was performed for each (see Supplementary Information, Figure S3). The difference in detection sensitivity between the bead-based and solution-based assays is depicted

in Figure 2.2. The ratio of the DNAzyme cleavage observed in the bead-based assay and that observed in the solution-based assay was calculated for each dilution for both the 1 hr and 12 hrs incubation times. The percentage of this ratio is shown on the Y-axis of Figure 2.2.

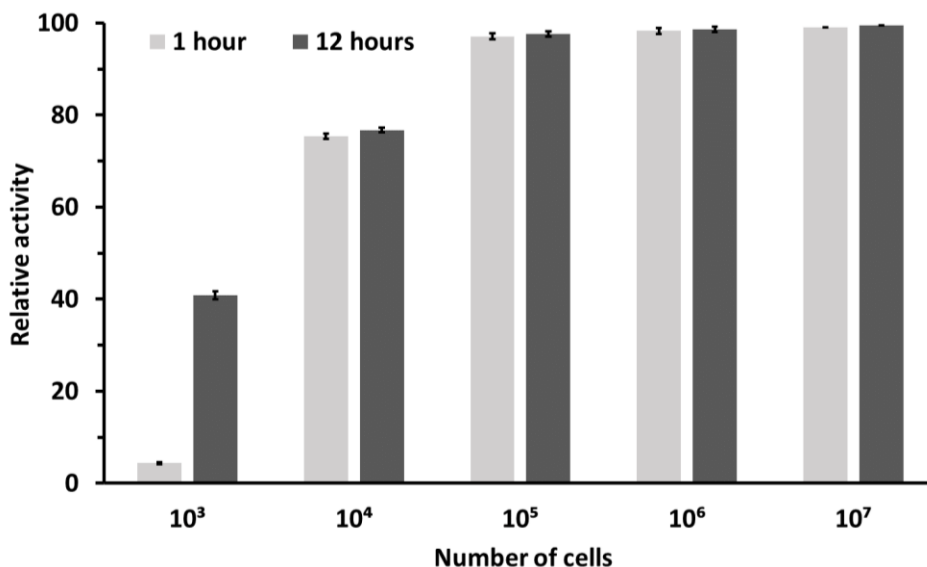


**Figure 2.2.** Comparison of Full DNAzyme detection sensitivity in solution-based and bead-based assays over 1 hr and 12 hr incubation time. The Y-axis indicates the relative activity, which is the percentage of the ratio of the DNAzyme cleavage in the bead-based assay to the DNAzyme cleavage in the solution-based assay. The X-axis indicates the number of *E. coli* cells used in each reaction mixture. The data shown in the charts are the average of three independent experiments and the error bars are based on the standard deviations of triplicate experiments.

As the results in Figure 2.2 show, the observed cleavage percentage in both assays is similar for cells numbering  $10^5$  or higher, though it is slightly lower for the bead-based assay. However, when the incubation time was increased to 12 hrs, the difference between the two assays decreased. With lower cell numbers ( $10^4$  and especially  $10^3$  cells), the cleavage percentage of the DNAzyme decreased at both time points in both assays, with the bead-based assay showing a greater decrease than the solution-based assay. Since the DNAzyme is restricted to the surface when it is immobilized on agarose beads, it is less accessible to its target cells, especially

when low amounts are present. As a result, the DNAzyme showed a greater response to the *E. coli* cells in the solution-based assay than in the bead-based assay. However, the magnitude of this difference was minimized by increasing the incubation time from 1 hr to 12 hrs. Based on the gel images visualized via Typhoon (Supplementary Information, Figure S3), our DNAzyme was able to detect as few as  $10^3$  *E. coli* cells in both the bead-based and solution-based assays. This was a promising result, as it provided further evidence that this solid-phase assay could be used in the development of an *E. coli*-detection biosensor.

### **2.3.3. Specificity of the Full DNAzyme in solution and immobilized on agarose beads**

The *E. coli* DNAzyme's specificity has been previously reported, and the data have confirmed that this probe is very specific for *E. coli* <sup>10,23,25,26,40–42</sup>. We enhanced our probe's cleavage activity by changing the catalytic domain's ligation site to the substrate and by eliminating the quencher from the substrate as well (see Supplementary Information, Figure S2). We were interested in investigating whether the DNAzyme's specificity would remain unaltered after the described modifications and after immobilization on agarose beads. To this end, a test was performed for the bead-based assay and the solution-based assay using two gram-negative bacteria, *Escherichia coli* K12 (*E. coli* K12; MG1655) and *Legionella pneumophila*, and two gram-positive bacteria, *Bacillus subtilis* 168 and *Listeria monocytogenes*. A single colony of each bacteria was grown overnight in Luria Broth (LB) growth media until the OD600 (optical density at 600 nm) of each cell culture reached ~1. CIMs ( $\sim 10^6$  cells) from each of the bacterial cultures were then prepared (as described in the Methods section) and tested with the DNAzyme

in the bead-based and solution-based assays. After 1 hr of incubation at room temperature, a 10% dPAGE analysis was conducted for each reaction mixture. The results are shown in Figure 2.3.

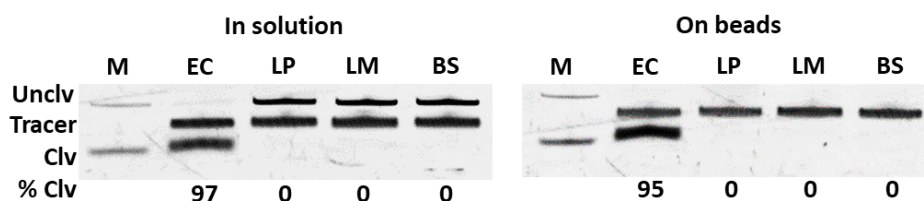


**Figure 2.3.** Specificity test of the Full DNAzyme using four different bacteria. The left image shows the solution-based assay, and the right image shows the bead-based assay. EC: *Escherichia coli*; LP: *Legionella pneumophila*; LM: *Listeria monocytogenes*; BS: *Bacillus subtilis*. Clv and Unclv represent the cleavage product and the full-length DNAzyme (which is uncleaved) respectively. The % Clv was calculated using the internal control, labeled “Tracer”, in the gel image (see Methods section for details).

As the results in Figure 2.3 show, only the *E. coli* CIM was able to induce cleavage in both assays, which means that our DNAzyme maintained its specificity toward *E. coli* cells, both in solution and after immobilization on agarose beads.

#### 2.3.4. Truncation analysis of the DNAzyme in solution and immobilized on agarose beads

The full DNAzyme sequence for *E. coli* (named IDE), contains 70 nucleotides and can be challenging to work with when it needs to be coupled with signal amplification strategies like RCA (rolling circle amplification). Conversely, the truncated DNAzyme sequence for *E. coli* (named sDE), contains only 23 nucleotides (these sequences are provided in Supplementary Information, Table S1). We tested the Full DNAzyme (including IDE and fluorogenic substrate) and the Short DNAzyme (including sDE and fluorogenic substrate) to compare their cleavage activity. The schematics of the Full and Short DNAzyme sequences are illustrated in Figure 2.4a.

Kinetic analysis was conducted for both DNAzymes for the bead-based and solution-based assays. Each reaction mixture contained  $10^5$  *E. coli* cells in order to prevent the DNAzyme

from becoming saturated with cells at the beginning of the reaction, which is an essential for being able to observe the differences in their cleavage activities at each time point. After being incubated at room temperature for the specified time points shown in Figure 2.4b, a 10% dPAGE analysis was conducted for each reaction mixture. The gel images are shown in Figure 2.4b.

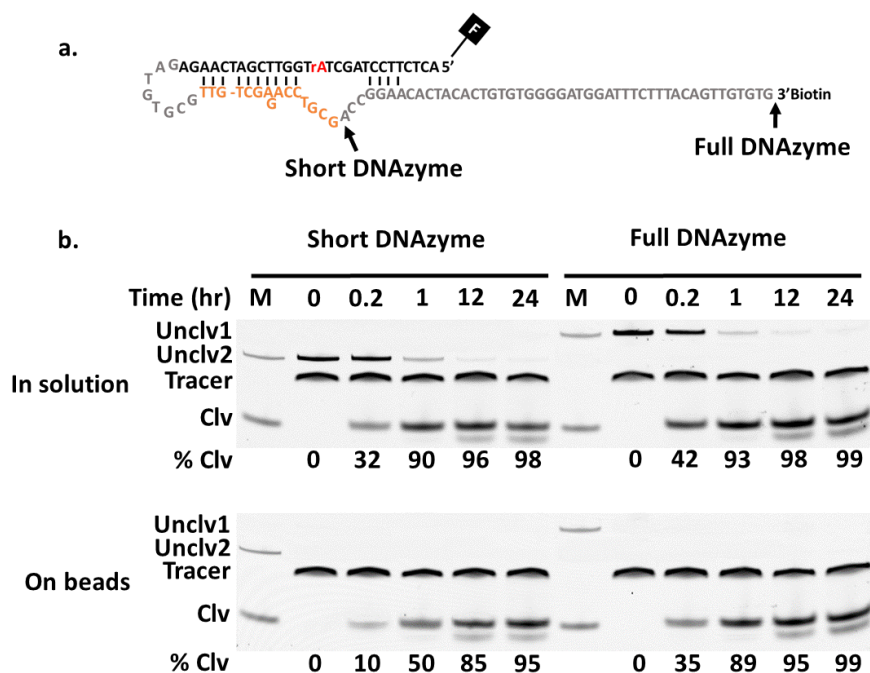


**Figure 2.4.** (a) Schematics of the Full and the Short DNAzyme sequences for *E.coli*. Both sequences start with 5' FAM and are modified with Biotin at 3' end of the sequences (the end point of the sequences is shown with the marker). The sequences are also provided in Supplementary Information, Table S1. (b) Truncation analysis of *E. coli* DNAzyme in solution (top panel) and immobilized on agarose beads (bottom panel). Clv in the gel images represents the cleavage product. Unclv1 and Unclv2 show the Full and Short DNAzymes (both uncleaved), respectively. The % Clv for each sample was calculated using the internal control, labeled “Tracer”, in the gel images (see Methods section for details).

As the results in Figure 2.4 show, the cleavage activity of both DNAzymes is comparable at each time point for the solution-based assay (the top panel of Figure 2.4b), with slightly better cleavage activity being observed for the Full DNAzyme. In the bead-based assay (the bottom panel of Figure 2.4b), the difference in cleavage activity between the two DNAzymes is much

more pronounced until 12 hrs of incubation, with faster activity being observed for the Full DNAzyme. This difference is likely attributable to the fact that the Full DNAzyme has more space between the catalytically active site and the immobilization site, which thus results in better activity during the bead-based assay.

Our results suggest that both the Full and Short DNAzymes could be useful in biosensor designs, as the difference between them was drastically reduced by increasing the incubation time to 24 hrs. Indeed, after 24 hrs of incubation, both had comparable cleavage percentages (see bottom line of each construct, the bottom panel of Figure 2.4b; *i.e.*, 95% vs. 99%). Thus, these constructs present researchers with two options. The first option is to use the Short DNAzyme in conjunction with signal amplification strategies like RCA in order to increase detection sensitivity. An additional advantage of this Short DNAzyme is that it is easier and more cost effective to synthesize than the Full sequence. The second option is to take advantage of the Full DNAzyme's faster cleavage activity, especially in bead-based assays.

### **2.3.5. Performance of the Full DNAzyme immobilized on agarose beads for the detection of *E. coli* in complex sample matrices**

The bead-based assay allows the uncleaved sequence attached to agarose beads to be separated from the cleavage fragment of the DNAzyme. This separation, which is not possible in solution-based assays, is essential in the development of biosensors because it minimizes non-specific background signals and amplifies target-based responses. The streptavidin-coated agarose beads used in this work have a nominal diameter of 35  $\mu\text{m}$  (between 20-50 microns),<sup>43</sup> which was

confirmed via confocal microscopy (Figure 2.5a), which also allowed to confirm the attachment of the FAM labeled DNAzyme to the surface of the beads.

Pierce Screw Cap Spin Columns containing polyethylene membranes with a 10  $\mu\text{m}$  pore size were used in the bead-based assay to separate the cleavage fragment of the DNAzyme from the uncleaved sequence. Common beverages such as milk, apple juice, and water were spiked with  $10^5$  *E. coli* cells. The milk and apple juice samples were diluted with reaction buffer to decrease their autofluorescence (See details in Methods section), and the same concentration of the Full DNAzyme (0.05  $\mu\text{M}$  in 100  $\mu\text{L}$  total reaction volume) was used in both the bead-based (in filter tubes mentioned above) and solution-based assays (in regular 1.5 mL microfuge tubes). For the control experiments, the samples were not spiked with *E. coli*. After a 1 hr reaction at room temperature, 10  $\mu\text{L}$  aliquots of each sample matrix—either with or without being subjected to filtration—and each reaction mixture from the both bead-based and solution-based assays were deposited on nitrocellulose paper. The autofluorescence of the controls and the fluorescence of the reaction mixtures were then imaged using a Chemidoc™ fluorescence imager (Bio-Rad).

The Spin Columns (900  $\mu\text{L}$  column volume) were attached to 5 mL syringes via a Luer-Lok adaptor (as illustrated in Figure 2.5b), and the solution was manually passed through the filter. This filtration method was able to effectively separate the intact (uncleaved) and cleaved sequences, with the cleavage product being collected as filtrate; thus, the employed filtration process can eliminate the need for specialized equipment and trained personnel to carry out separation by centrifugation. The representative fluorescent image of all samples is illustrated in

Figure 2.5c. Additionally, the fluorescence signal of each sample was measured using a TECAN M1000 plate reader (see Supplementary Information, Figure S4).

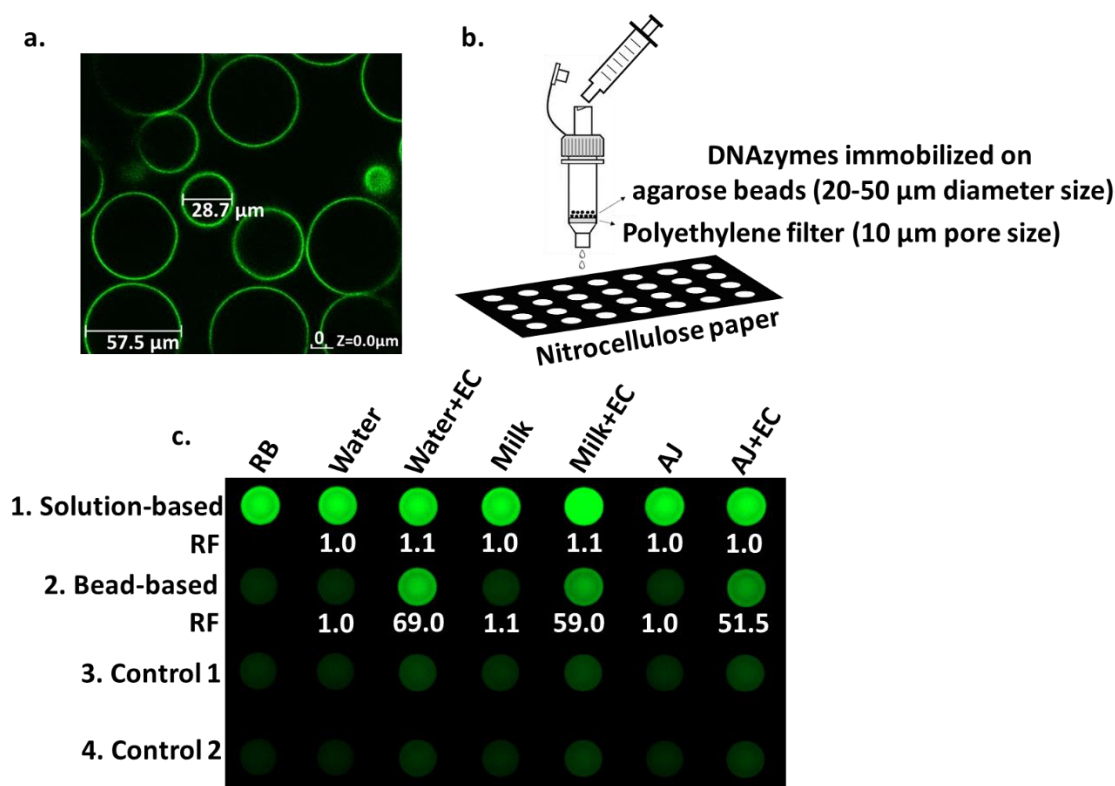


**Figure 2.5.** (A) Confocal microscopy of the Full DNAzyme immobilized on agarose beads. This image confirms the attachment of the biotinylated DNAzyme to the surface of streptavidin-coated agarose beads. (B) Schematic of the bead-based biosensor. (C) Performance of the bead-based biosensor in detecting *E. coli* in water, milk and apple juice samples (Water: water alone; Water+EC: water spiked with *E. coli*; Milk: diluted milk alone; Milk+EC: diluted milk spiked with *E. coli*; AJ: diluted apple juice alone; AJ+EC: diluted apple juice spiked with *E. coli*). Row 1 presents the maximum fluorescence signal obtained during in the solution-based assay for each matrix with and without *E. coli*. Row 2 presents the cleavage event signal in the bead-based assay. Row 3 shows the autofluorescence of control samples without DNAzyme and beads. Row 4 shows the autofluorescence of the control samples without DNAzyme and beads after subjection to filtration. RF is the relative fluorescence calculated for Row 1 and Row 2 by dividing the fluorescence signal of each zone by the fluorescence signal of the reaction buffer zone.

As the results in Figure 2.5c show, the maximum fluorescence signal was observed in the solution-based assay, both with and without *E. coli*. Other previously reported solution-based



assays have employed a fluorophore-quencher pair system to monitor the molecular-recognition event and subsequent cleavage<sup>10,23,25,40</sup>; however, with the relatively simpler design used in this current work, the substrate is just FAM labeled (it does not have the additional quencher modification). The relative fluorescence (RF), which is calculated by dividing the fluorescence signal of each zone by the fluorescence signal of the reaction buffer zone, was ~1 for all samples in the solution-based assay. In contrast, we know that the signal observed in the bead-based assay is solely the product of cleavage due to the presence of *E.coli*, as only the cleaved fragment of the DNAzyme is able to pass through the filter. Moreover, the autofluorescence of the samples in Control group 2 was much lower than the signal generated in the bead-based assay in presence of *E. coli* (Row 2 vs. Row 4, Figure 2.5c), which indicates that the signal observed in the bead-based assay is solely the product of a cleavage event in presence of *E. coli*. This simple partitioning step decreases background interference and also allows the filtrate to be concentrated, thereby amplifying the signal generated by the cleavage event. The proposed bead-based biosensor system was able to identify the samples spiked with *E. coli* by showing an obvious increase in their fluorescence signals, which is a significant achievement as this would allow non-experts to detect the presence of *E.coli* using a simple hand-held fluorescence device.

#### **2.4. Conclusion**

In this chapter, we have documented the development of a robust, simple, sensitive, and cost-effective bead-based assay capable of detecting *E. coli* via an RNA-cleaving DNAzyme. Our simple-to-perform assay eliminates the need for specialized equipment and trained personnel by combining the advantages of agarose beads, which are cheap and widely available, and an easy-

to-implement filtration step. These advantages make the proposed bead-based bacterial-detection assay highly attractive for field applications, especially in resource-limited regions. In addition to its ease of use, our bead-based sensor is very fast and is capable of producing a strong fluorescence signal in as few as 2.5 min after coming into contact with the target bacteria. Furthermore, the sensor's simple partitioning step successfully decreases non-specific background noise, which in turn allows for the sensitive detection of *E. coli* in water samples, or complex sample matrices, such as milk and apple juice.

Finally, it is worth noting that DNAzyme probes can be isolated through *in vitro* selection to react to different bacteria. Given this, the proposed bead-based assay, which was designed based on an RNA-cleaving DNAzyme, could be easily extended to detect a wide range of bacterial targets by utilizing the appropriate DNAzyme.

## **2.5. Materials and Methods**

### **2.5.1. Chemical reagents**

All DNA oligonucleotides and the RNA-containing fluorogenic substrate were purchased from Integrated DNA Technologies (IDT, Coralville, IA, USA) and were purified via standard 10% denaturing (8 M urea) polyacrylamide gel electrophoresis (dPAGE). The sequences and functions of all synthetic oligonucleotides used in this study are provided in Supplementary Information, Table S1. ATP, T4 DNA ligase, and T4 polynucleotide kinase (PNK), along with their respective buffers, were purchased from Thermo Scientific (Ottawa, ON, Canada). Nitrocellulose paper (HF120), which was backed with a thin plastic layer on one side, was purchased from GE Healthcare, Canada. Reduced graphene oxide was prepared according to a

method previously reported by our lab <sup>44</sup>. 1.5 µm streptavidin-coated magnetic beads (BioMag-SA) were purchased from Bangs Laboratories, Inc., while 20-50 µm streptavidin-coated agarose beads were obtained from TriLink Biotechnologies, Inc. Spin-X® Centrifuge Tube Filters containing cellulose acetate membranes with 0.22 µm pore size were obtained from VWR International (Mississauga, ON, Canada). Pierce Screw Cap Spin Columns containing polyethylene membranes with a 10 µm pore size were purchased from Thermo Scientific. Milk (Neilson™ skim milk) and apple juice (Minute Maid) were purchased from a local supermarket, while the water used in the experiments was purified with a Milli-Q Synthesis A10 water-purification system. All other chemicals were purchased from Sigma-Aldrich (Oakville, Canada) and were used without further purification.

### **2.5.2. Bacterial cells preparation**

Two gram-negative bacteria, *Escherichia coli* K12 (*E. coli* K12; MG1655) and *Legionella pneumophila*, and two gram-positive bacteria, *Bacillus subtilis* 168 and *Listeria monocytogenes*, were used in this work.

In order to determine the number of *E. coli* cells in the experiments, the *E. coli* colonies were first transferred to Luria Broth (LB) agar plates before being incubated for 14 h at 37 °C. Following incubation, a single colony was taken and inoculated into 2 mL of LB and grown for 14 h at 37 °C with continuous shaking at 250 rpm (the culture will reach an OD<sub>600</sub>~1). 10-fold serial dilution was then conducted and 100 µL of the diluted solutions was then spread onto LB agar plates (done in triplicate) and incubated at 37°C for 16 h. Finally, the colonies were counted and averaged in order to obtain the *E. coli* cell concentration.

The crude intracellular mixture (CIM) of *E. coli* K12, which contains more target protein than the crude extracellular mixture (CEM) of *E. coli* K12<sup>23,40</sup>, was prepared by centrifuging 1 mL of each dilution at 11,000 g for 5 min at 4°C. Next, the clear supernatant was discarded, and the cell pellet was re-suspended in 100 µL of double-deionized water (ddH<sub>2</sub>O) and heated at 65 °C for 5 min. The heat-treated cell suspension was then vortexed to dissolve the cell pellet completely and stored at -20 °C. Based on the number of cells needed for each experiment, a relevant CIM of *E. coli* was used in the experiments.

The CIMs for the other above-mentioned bacteria were made following a similar procedure: first, the bacterial colonies were plated on LB agar plates and incubated at 37 °C for 14 h; second, a single colony was taken and inoculated into 2 mL of LB and grown at 37 °C with continuous agitation at 250 rpm until the OD<sub>600</sub> (optical density at 600 nm) of each cell culture reached ~1; third, 1 mL of each bacterial culture was centrifuged at 11,000 g for 5 min at 4°C; and finally, the clear supernatant was removed and the cell pellet was re-suspended in 100 µL of ddH<sub>2</sub>O and heated at 65 °C for 5 min. The resultant heated solution was then used for the specificity experiment

### **2.5.3. Preparation of DNazymes**

IDE (long DNzyme sequence for *E. coli* K12) and sDE (short DNzyme sequence for *E. coli* K12) were enzymatically ligated to an FS (Fluorogenic substrate) in order to generate the complete DNzyme sequences, that were used in our experiments. The sequences are provided in Supplementary Information, Table S1. Since both DNzymes were synthesized using similar protocols, IDE or sDE will both be written as DE here. Briefly, this protocol was as follows: 2

nmol of DE was phosphorylated in 200  $\mu\text{L}$  of  $1\times$  PNK buffer A containing 2 mM ATP (final concentration) with 40 U (units) of PNK enzyme at 37  $^{\circ}\text{C}$  for 40 min. The enzyme was inactivated by heating the reaction mixture at 90  $^{\circ}\text{C}$  for 5 min and then cooling it to room temperature for 15 min. Next, an equal number of FS and LT were added to the reaction mixture. The mixture was then heated to 90  $^{\circ}\text{C}$  for 1 min and then cooled back to room temperature for 15 min. Once the mixture had cooled, 40  $\mu\text{L}$  of  $10\times$  DNA ligase buffer and 40 U of T4 DNA Ligase were added and the final volume was adjusted to 400  $\mu\text{L}$  by adding ddH<sub>2</sub>O. After incubation at room temperature for 2 h, the DNA molecules were isolated by ethanol precipitation and the ligated DNA molecules were purified via 10% dPAGE. After being dissolved in ddH<sub>2</sub>O, the DNAzyme concentration was measured using a DeNovix DS-11+ Spectrophotometer and adjusted to 1  $\mu\text{M}$  via dilution in ddH<sub>2</sub>O. Finally, the DNAzymes solutions were stored at  $-20^{\circ}\text{C}$  until use in the experiments.

#### **2.5.4. Immobilization of DNAzymes onto agarose beads**

20  $\mu\text{L}$  of streptavidin-coated agarose beads were washed in 100  $\mu\text{L}$  of  $1\times$  reaction buffer ( $1\times$  RB; 50 mM HEPES, pH 7.5, 150 mM NaCl, 15 mM MgCl<sub>2</sub>) in Spin-X® Centrifuge Tube Filters at 4,000 g for 5 min at 4 $^{\circ}\text{C}$ . Once washed, the solution was discarded and the filter containing the solid beads (10  $\mu\text{L}$  of beads remained on top of the filter after centrifugation) was transferred to a new 1.5 mL microfuge tube. 5 pmol of the biotinylated DNAzyme (5  $\mu\text{L}$  of 1  $\mu\text{M}$ ), 50  $\mu\text{L}$  of  $2\times$  RB (double the concentration of  $1\times$  RB) and 35  $\mu\text{L}$  of ddH<sub>2</sub>O were then added to the 10  $\mu\text{L}$  of washed beads to make 100  $\mu\text{L}$  of total reaction volume. Next, the reaction mixture was incubated at room temperature for 1 h in order to facilitate the streptavidin-biotin interaction. Once this

time period had elapsed, the tube was centrifuged at 4,000 g for 5 min at 4°C in order to remove the unattached DNAzymes. After centrifuging, the beads were washed three times in 100 µL 1× RB in order to remove the non-specific binded DNAzymes. Since the DNAzymes have a fluorogenic substrate, the number of DNAzymes attached to the beads can be determined by measuring the fluorescent intensity of DNAzymes remaining in the solution phase after immobilization using a TECAN M1000 plate reader. After three washes, the immobilized DNAzymes on the beads in the filter were ready for use in the cleavage test.

#### **2.5.5. Internal normalization for calculating the amount of cleavage product**

Internal normalization for all of the experiments in this work was done by adding a known amount of ssDNA that was labelled with fluorophore to all of the samples (the fluorophore sequence is provided in Supplementary Information, Table S1, named “Tracer”). In the solution-based assay, the DNA samples were subjected to 10% dPAGE for DNA separation and the bands were then visualized in the gel using Typhoon 9200 (GE Healthcare); this revealed two cleaved and uncleaved DNA bands. The amount of cleavage product and the cleavage percentage were calculated by comparing the intensity of these two bands using ImageQuant software (Molecular Dynamics). Conversely, the gel images for the assay using immobilized DNAzymes on agarose beads revealed just the cleaved bands, as the uncleaved DNAzymes became attached to the beads. By having an internal control, it is possible to calculate the amount of cleavage product in each sample by comparing the intensity of the cleaved band to its own tracer band. To confirm the accuracy of this method, the internal control was added to the solution-phase samples. In the solution-based assay, the same amount of cleavage product was obtained both by comparing the

intensities of the cleaved and uncleaved bands, and also by comparing the intensities of the cleaved and tracer bands. The amount of cleavage product in the solid-phase samples can also be determined using this method, while the cleavage percentage can be obtained by dividing the amount of cleavage product by the amount of DNAzymes attached to the beads. To ensure consistency and improve control, the same amount of ssDNA was added to all of the samples in the bead-based and solution-based assays. It was possible to confirm the accuracy of the calculations using just 1 gel image; the gel images of the bead-based samples in Figure 2.1 are also included in the last lane of their related solution-based samples (labeled SC in the right part of Figure 2.1a and 2.1b).

#### **2.5.6. Kinetic analysis of the Full DNAzyme's activity in solution**

Two reactions were set up: one with  $10^6$  *E. coli* cells and another with  $10^4$  *E. coli* cells. The cleavage reaction was conducted in 100  $\mu\text{L}$  of  $1\times$  RB that contained 5 pmol of the Full DNAzyme, 3 pmol of tracer, and either  $10^6$  or  $10^4$  *E. coli* cells. At certain time points, which are shown in Figure 2.1 (0, 2.5, 5, 7.5, 10, 20, 30, 60, and 120 min), 10  $\mu\text{L}$  were withdrawn from each reaction mixture and quenched by adding 10  $\mu\text{L}$  of  $2\times$  quenching buffer ( $2\times$  QB; 200 mM EDTA, 16 M urea; 100 mM Tris-borate; 0.6 M sucrose; 0.1% (w/v) SDS; 0.025 % (w/v) xylene cyanol; and 0.025 % (w/v) bromophenol blue, pH 8.3). 10  $\mu\text{L}$  of each sample was then analyzed by 10% dPAGE, which was followed by fluorescence scanning with Typhoon and quantification with ImageQuant software as described above. These experiments were repeated three times. After averaging the data obtained from the triplicate experiments and fitting a curve, the slope of

the linear region of the curves (0-5 min) was calculated, which represented the initial rate of cleavage percentage.

### **2.5.7. Kinetic analysis of the Full DNAzyme's activity immobilized on agarose beads**

As in the solution-based assay, two reaction conditions were assessed: one with  $10^6$  *E. coli* cells and another with  $10^4$  *E. coli* cells. After immobilizing the Full DNAzyme onto the agarose beads and subjecting them to three washings (as describe above), 3 pmol tracer and either  $10^6$  or  $10^4$  *E. coli* cells were added to the immobilized DNAzyme on the beads (final reaction volume = 100  $\mu$ L in  $1 \times$  RB). Since the reaction mixture should be centrifuged after each time point in order to separate the solution from the beads, a separate reaction mixture was prepared for each time point. After centrifugation at each time point, 10  $\mu$ L from each reaction mixture were mixed with 10  $\mu$ L of  $2 \times$  QB, which was followed by 10% dPAGE analysis as described above. This experiment was conducted in triplicate and the initial rate of cleavage percentage was calculated as described above.

### **2.5.8. Detection sensitivity of the Full DNAzyme in solution and immobilized on agarose beads**

To evaluate the detection sensitivity of the DNAzyme in the solution and the DNAzyme immobilized on the surface of beads, different numbers of *E. coli* cells were used. The CIMs of *E. coli* containing  $10^7$ ,  $10^6$ ,  $10^5$ ,  $10^4$ ,  $10^3$ ,  $10^2$ , 10, and 1 cell were prepared as described above. For each number of cells, two reaction mixtures were prepared: one for 1 hr incubation time and one for 12 hrs incubation time. Each reaction mixture contained a relevant CIM of *E. coli*, 5 pmol DNAzyme, and 3 pmol tracer in 100  $\mu$ L of  $1 \times$  RB. For the bead-based assay, 3 pmol tracer



and a relevant CIM of *E. coli* were added to the immobilized DNAzyme on agarose beads to make a final reaction volume of 100  $\mu$ L. Each reaction mixture was incubated at room temperature for either 1 hr or 12 hr, which was followed by 10% dPAGE analysis as described above. This experiment was conducted in triplicate.

#### **2.5.9. Specificity of the Full DNAzyme in solution and immobilized on agarose beads**

Two gram-negative bacteria, *Escherichia coli* K12 (*E. coli* K12; MG1655) and *Legionella pneumophila*, and two gram-positive bacteria, *Bacillus subtilis* 168 and *Listeria monocytogenes*, were used to evaluate the specificity of the DNAzyme. CIMs ( $\sim 10^6$  cells) from each of the bacterial cultures were prepared as described above. The cleavage reactions were conducted in the same manner as the sensitivity tests for the bead-based and solution-based assays, only this time different bacteria was used rather than different *E. coli* concentrations. After incubation, each reaction mixture was left to incubate at room temperature for 60 min before conducting a 10% dPAGE analysis as described above.

#### **2.5.10. Truncation analysis of the DNAzyme in solution and immobilized on agarose beads**

To compare the cleavage activity of the full DNAzyme sequence and its truncated version (named Full DNAzyme and Short DNAzyme, respectively, in Supplementary Information, Table S1), kinetic analysis was conducted for both the bead-based and solution-based assays.  $10^5$  *E. coli* cells were used to prevent the DNAzymes from becoming saturated with cells at the beginning of the reaction, and to better observe the differences in cleavage activity after each time point. For each sequence, the cleavage reactions were conducted in the same manner as the kinetic analysis tests for the bead-based and solution-based assays. However, this analysis

differed slightly as it used the different time points specified in Figure 2.4b, as well as  $10^5$  *E. coli* cells. The sequences were analyzed via 10% dPAGE analysis procedure (as described above), and the experiments were conducted in triplicate.

#### **2.5.11. Performance of the Full DNAzyme immobilized on agarose beads for the detection of *E. coli* in complex sample matrices**

Since the agarose beads have a relatively large nominal diameter of 20-50 microns, we can use them with filter tubes that have larger pore sizes. Thus, filter clogging is not an issue in complex samples with higher numbers of *E. coli* cells. For this research, Pierce Screw Cap Spin Columns containing polyethylene membranes with a 10  $\mu\text{m}$  pore size were used to separate the cleavage fragment of the DNAzyme from the uncleaved sequence in the bead-based assay; significantly, this is not possible in the solution-based assay. In the bead-based assay, the background signal is eliminated, which allows *E. coli* to be detected as a result of the sole signal produced by the cleavage event. Common beverages such as milk (Neilson™ skim milk), apple juice (Minute Maid), and water were chosen for this study.

Since we are tracking the fluorescence signal in this assay, it is important to correct the background fluorescence in complex samples, such as milk and apple juice. It has been previously reported that 12.5% milk and 25% apple juice have low background fluorescence signals and suitable pH for DNAzyme performance tests<sup>25</sup>. For the tests, these dilutions of milk and apple juice were prepared by mixing the samples with the reaction buffer and spiking the resultant mixture with CIM of *E. coli*; for the controls, on the other hand, the milk and apple juice were only mixed with the reaction buffer. The cleavage reaction for the solution-based

assay was conducted in a regular 1.5 mL microfuge tube with 100  $\mu\text{L}$  of  $1\times$  RB containing 5 pmol DNAzyme and  $10^5$  *E. coli* cells. In contrast, the bead-based assay was conducted in the above-described filter tubes, but using the same solution. Each reaction mixture was incubated at room temperature for 60 min. As illustrated in Figure 2.5b, a syringe can be used to push the solution out from the bottom of the filter tube, rather than having to rely on centrifugation. 10  $\mu\text{L}$  of each sample, with and without filtration, and for each reaction mixture from the bead-based and solution-based assays were then deposited on nitrocellulose paper. Nitrocellulose paper was chosen for this experiment due to its low background fluorescence and its prevention of aqueous sample diffusion<sup>25</sup>. The wax-printing technique was used (using a Xerox ColorQube 8570N solid wax printer) to produce a 96-microzone paper plate with test zones measuring 4 mm in diameter. The image in Figure 2.5c was obtained using a Chemidoc<sup>TM</sup> fluorescence imager (Bio-Rad). Additionally, a TECAN M1000 plate reader was used to measure the fluorescence signal of all samples, as well as to calculate their relative fluorescence (RF).

## 2.6. Appendix

### Supplementary Information

#### Development of a bead-based assay for the detection of *E.coli* using DNAzymes

Sahar Esmaeili Samani<sup>1,2</sup>, Erin M. McConnell<sup>2</sup>, Dingran Chang<sup>2</sup>, Carlos D.M. Filipe<sup>1</sup> and  
Yingfu Li<sup>2,\*</sup>

1. *Department of Chemical Engineering, McMaster University, 1280 Main St. W., Hamilton, ON  
L8S 4L7, Canada.*

2. *Department of Biochemistry and Biomedical Sciences, McMaster University, 1280 Main St.  
W., Hamilton, ON L8S 4K1, Canada.*

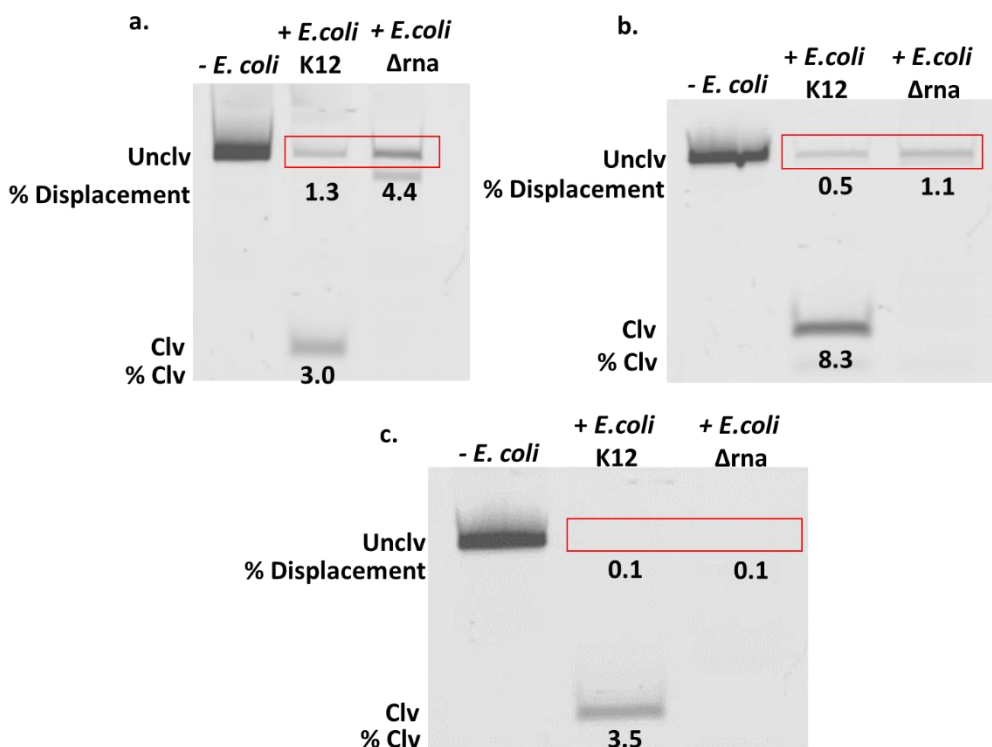


**Figure S1.** Immobilization of *E. coli* DNase I onto three different materials: (a) Reduced graphene oxide; (b) Magnetic beads; and (c) Agarose beads. In each gel image, the left, middle, and right columns indicate samples with no *E. coli* cells, the presence of *E. coli* K12, and the presence of *E. coli* Δrna (this bacteria is not a specific protein target for the DNase I, so it does not induce the cleavage activity of the DNase I). As gel images show, agarose beads yielded the highest signal-to-background ratio (comparing  $3/1.3 = 2.3$ ,  $8.3/0.5 = 16.6$ ,  $3.5/0.1 = 35$  for reduced graphene oxide, magnetic beads, and agarose beads, respectively). Note that the higher cleavage exhibited by magnetic beads was due to the higher number of *E. coli* cells (5000 *E. coli* cells) than were used with reduced graphene oxide and agarose beads (2000 *E. coli* cells).

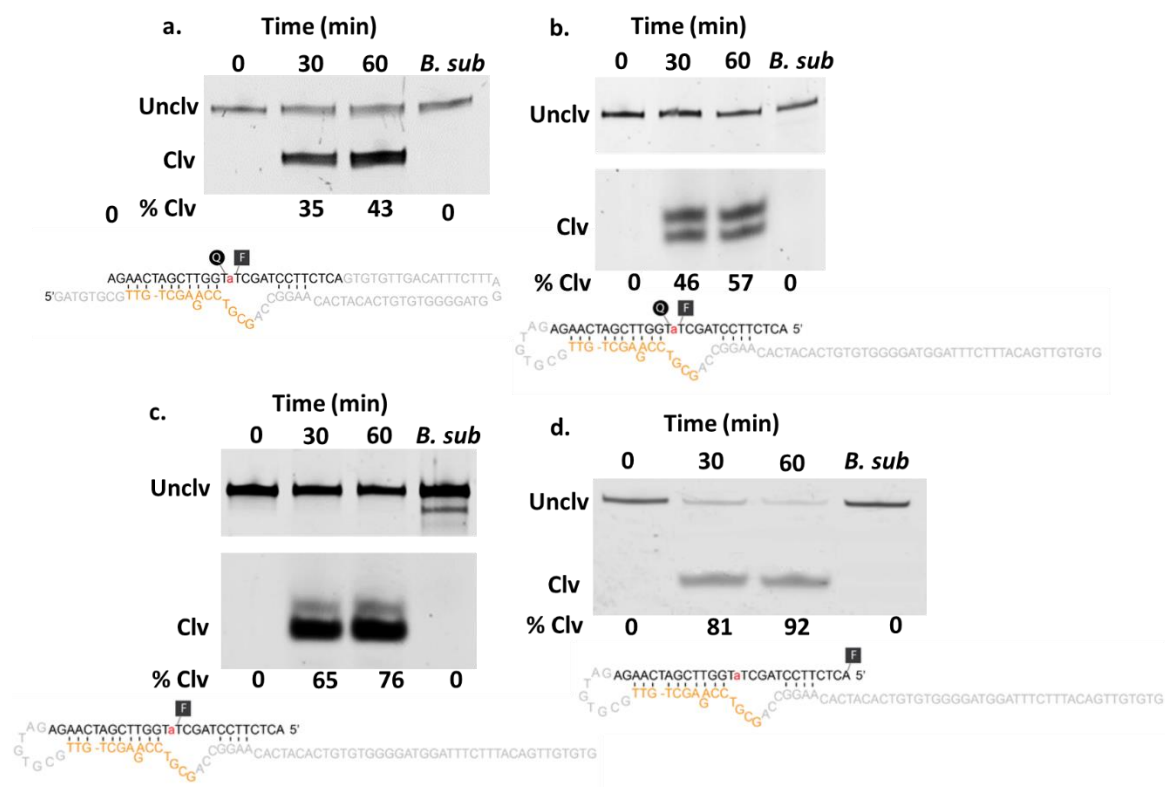


**Figure S2.** Differences between previously reported *E. coli* DNase I and our probe. (a) The previously reported *E. coli* DNase I was ligated to the FQ substrate at its 3' end<sup>40</sup>. (b) Also previously investigated, the DNase I was ligated to the FQ substrate at its 5' end<sup>26</sup>. (c) The DNase I was ligated to the FAM-labeled substrate at its 5' end (internal modification). (d) The DNase I was ligated to the FAM-labeled substrate at its 5' end (external modification). The aforementioned probe for *E. coli* was used in this work because it resulted in the best cleavage activity. *Bacillus subtilis* bacterium (*B. sub*) was used as the control in each experiment.

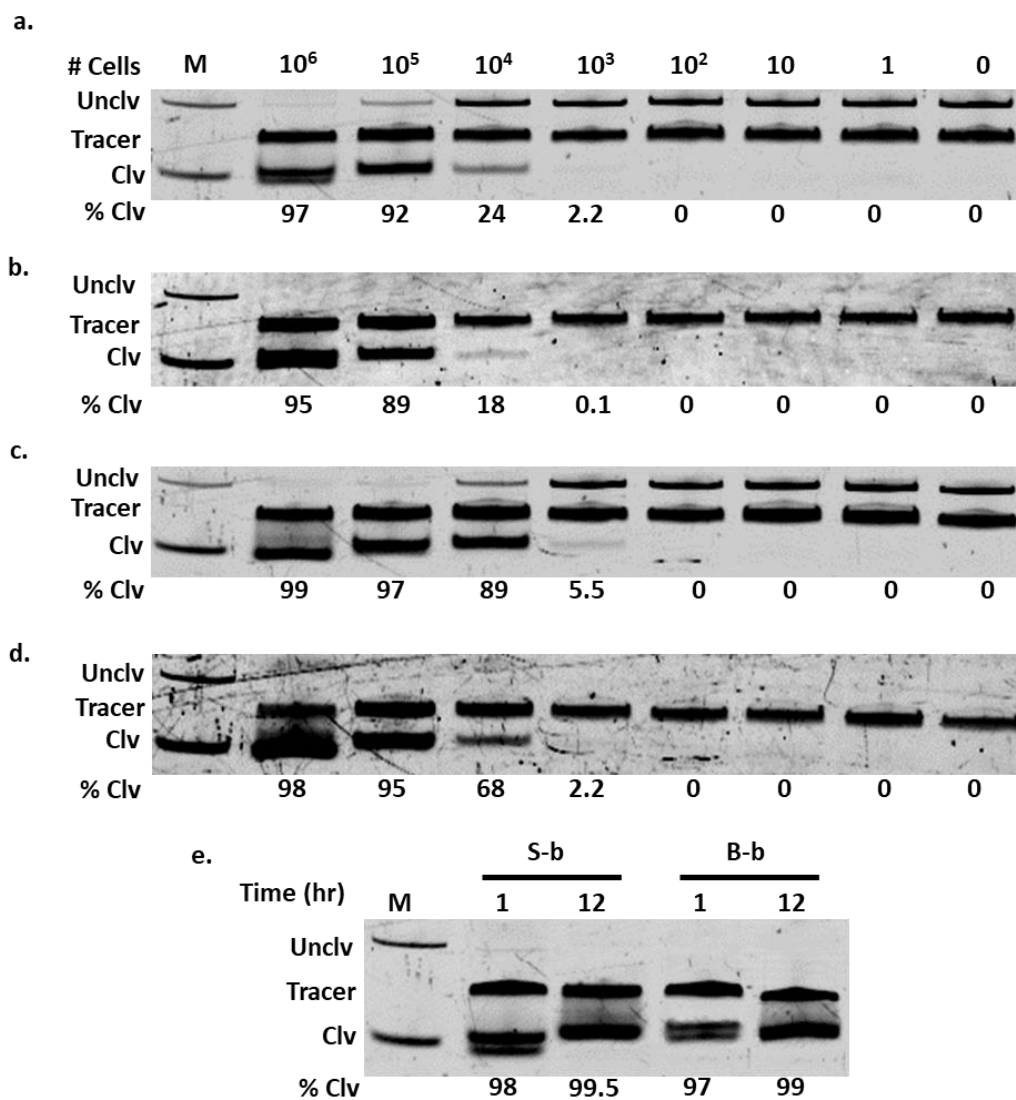


**Figure S3.** 10% dPAGE analysis of sensitivity test for creating Figure 2.2. (a) Solution-based assay, 1 hr incubation time. (b) Bead-based assay, 1 hr incubation time. (c) Solution-based assay, 12 hr incubation time. (d) Bead-based assay, 12 hr incubation time. (e) Similar experiment using  $10^7$  *E. coli* cells. S-b and B-b represent the solution-based and bead-based assays, respectively. The % Clv for each sample was calculated using the internal control, which is labeled, “Tracer”, in the gel images (see Methods section in the main text for details).

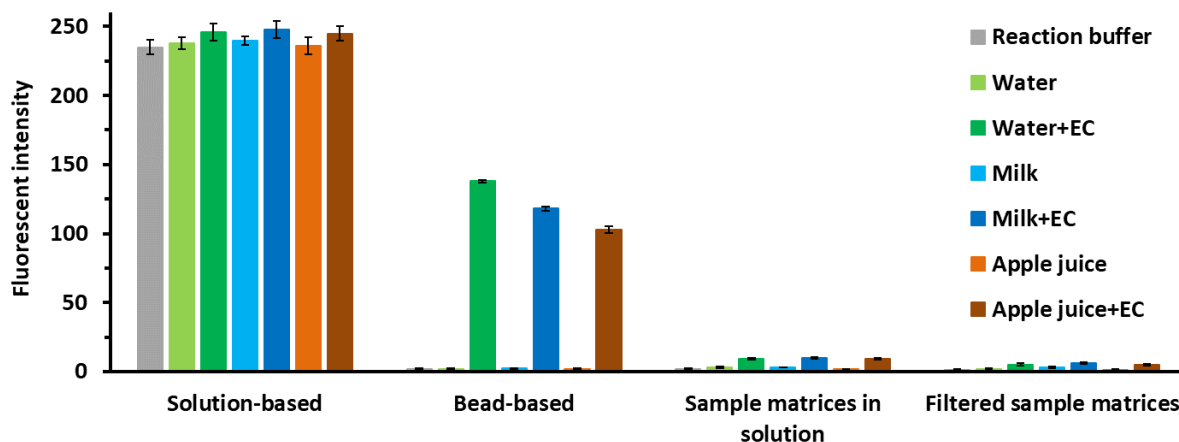


**Figure S4.** Autofluorescence signal of the controls, and the fluorescence signals of the reaction mixtures represented in Figure 2.5c. EC stands for *E. coli*, and the reaction mixtures are defined in the legend of Figure 2.5. The error bars are based on the standard deviations of the experiments, which were performed in triplicate.



**Table S1.** The sequences of and modifications to all oligonucleotides used in this work.

Name	Labels	Sequence	Note
IDE	3' Biotin-TEG	5'-GATGTGCGTTGTCGAGACCTGCG ACCGGAACACTACACTGTGTGGGG ATGGATTTCTTTACAGTTGTGTG-3'	Long DNAzyme sequence for <i>E. coli</i> K12
sDE	3' Biotin-TEG	5'-GATGTGCGTTGTCGAGACCTGCG-3'	Short DNAzyme sequence for <i>E. coli</i> K12
FS	5' 6-FAM (6-Carboxyfluorescein), Riboadenosine ( rA)	5'-ACTCTTCCTAGCTrATGGTTCGATCAAGA-3'	Fluorogenic substrate
LT	None	5'-CAAGACGCACATCTC TTGAT CGAACC-3'	Ligation Template for ligating FS to IDE or sDE
Tracer	5' 6-FAM (6-Carboxyfluorescein)	5' -TAG GGG GTG CCC GTA AGG AAG GAT CGT GAG GCG GT	Internal control
Full DNAzyme	3' Biotin-TEG, 5' 6-FAM	5'-ACTCTTCCTAGCTrATGGTTCGATCAAGA GATGTGCGTTGTCGAGACCTGCG ACCGGAACACTACACTGTGTGGGG ATGGATTTCTTTACAGTTGTGTG-3'	Complete DNAzyme sequence including IDE and FS
Short DNAzyme	3' Biotin-TEG, 5' 6-FAM	5'-ACTCTTCCTAGCTrATGGTTCGATCAAGA GATGTGCGTTGTCGAGACCTGCG-3'	Truncated DNAzyme sequence including sDE and FS

## 2.7. References

1. Ramachandran, A., Flinchbaugh, J., Ayoubi, P., Olah, G. A. & Malayer, J. R. Target discrimination by surface-immobilized molecular beacons designed to detect *Francisella tularensis*. *Biosens. Bioelectron.* **19**, 727–736 (2004).
2. Dalavoy, T. S. *et al.* Immobilization of DNAzyme catalytic beacons on PMMA for Pb<sup>2+</sup> detection. *Lab Chip* **8**, 786–793 (2008).
3. Sassolas, A., Blum, L. J. & Leca-Bouvier, B. D. Immobilization strategies to develop enzymatic biosensors. *Biotechnol. Adv.* **30**, 489–511 (2012).
4. Pedano, M. L. & Rivas, G. A. Adsorption and electrooxidation of nucleic acids at carbon nanotubes paste electrodes. *Electrochem. commun.* **6**, 10–16 (2004).
5. Stanciu, L., Won, Y.-H., Ganesana, M. & Andreescu, S. Magnetic Particle-Based Hybrid Platforms for Bioanalytical Sensors. *Sensors* **9**, 2976–2999 (2009).
6. Malhotra, B. D. & Chaubey, A. Biosensors for clinical diagnostics industry. *Sensors Actuators, B Chem.* **91**, 117–127 (2003).
7. Wernette, D. P. *et al.* Incorporation of a DNAzyme into Au-coated nanocapillary array membranes with an internal standard for Pb(II) sensing. *Analyst* **131**, 41–47 (2006).
8. Levicky, R., Herne, T. M., Tarlov, M. J. & Satija, S. K. Using self-assembly to control the structure of DNA monolayers on gold: A neutron reflectivity study. *J. Am. Chem. Soc.* **120**, 9787–9792 (1998).
9. Swearingen, C. B. *et al.* Immobilization of a catalytic DNA molecular beacon on Au for Pb(II) detection. *Anal. Chem.* **77**, 442–448 (2005).
10. Yousefi, H., Ali, M. M., Su, H. M., Filipe, C. D. M. & Didar, T. F. Sentinel Wraps: Real-Time Monitoring of Food Contamination by Printing DNAzyme Probes on Food Packaging. *ACS Nano* **12**, 3287–3294 (2018).
11. Andreescu, S. & Marty, J. L. Twenty years research in cholinesterase biosensors: From basic research to practical applications. *Biomol. Eng.* **23**, 1–15 (2006).
12. Mello, L. D. & Kubota, L. T. Review of the use of biosensors as analytical tools in the food and drink industries. *Food Chem.* **77**, 237–256 (2002).
13. ZHAO, X. H. *et al.* Recent Progress of DNAzyme-Nanomaterial Based Biosensors. *Chinese J. Anal. Chem.* **43**, 1611–1619 (2015).

14. Li, Y. & Breaker, R. R. Deoxyribozymes: New players in the ancient game of biocatalysis. *Curr. Opin. Struct. Biol.* **9**, 315–323 (1999).
15. Liu, J., Cao, Z. & Lu, Y. *Functional Nucleic Acid Sensors Functional Nucleic Acid Sensors*. **109**, (2009).
16. Navani, N. K. & Li, Y. Nucleic acid aptamers and enzymes as sensors. *Curr. Opin. Chem. Biol.* **10**, 272–281 (2006).
17. Breaker, R. R. & Joyce, G. F. A DNA enzyme that cleaves RNA. *Chem. Biol.* **1**, 223–229 (1994).
18. Gysbers, R.; Tram, K.T.; Manochery, S.; Chang, D.; Li, Y. *Selection and application of catalytically active oligonucleotides*. (Pan Stanford: Boca Raton, FL, USA, 2016).
19. Mok, W. & Li, Y. Recent progress in nucleic acid aptamer-based biosensors and bioassays. *Sensors* **8**, 7050–7084 (2008).
20. Gong, L. *et al.* DNAzyme-based biosensors and nanodevices. *Chem. Commun.* **51**, 979–995 (2015).
21. Tram, K., Kanda, P. & Li, Y. Lighting Up RNA-cleaving DNAzymes for biosensing. *J. Nucleic Acids* **2012**, (2012).
22. Liu, M., Chang, D. & Li, Y. Discovery and Biosensing Applications of Diverse RNA-Cleaving DNAzymes. *Acc. Chem. Res.* **50**, 2273–2283 (2017).
23. Ali, M. M., Aguirre, S. D., Lazim, H. & Li, Y. Fluorogenic DNAzyme probes as bacterial indicators. *Angew. Chemie - Int. Ed.* **50**, 3751–3754 (2011).
24. Santoro, S. W. & Joyce, G. F. Mechanism and utility of an RNA-cleaving DNA enzyme. *Biochemistry* **37**, 13330–13342 (1998).
25. Ali, M. M. *et al.* A Printed Multicomponent Paper Sensor for Bacterial Detection. *Sci. Rep.* **7**, 1–10 (2017).
26. Tram, K., Kanda, P., Salena, B. J., Huan, S. & Li, Y. Translating bacterial detection by DNAzymes into a litmus test. *Angew. Chemie - Int. Ed.* **53**, 12799–12802 (2014).
27. Liu, J. & Lu, Y. A colorimetric lead biosensor using DNAzyme-directed assembly of gold nanoparticles. *J. Am. Chem. Soc.* **125**, 6642–6643 (2003).
28. Chang, D. *et al.* Integrating Deoxyribozymes into Colorimetric Sensing Platforms. *Sensors (Basel)*. **16**, (2016).

29. Aguirre, S. D., Ali, M. M., Kanda, P. & Li, Y. Detection of Bacteria Using Fluorogenic DNAzymes. *J. Vis. Exp.* 1–8 (2012). doi:10.3791/3961
30. Xiao, Y., Rowe, A. A. & Plaxco, K. W. Electrochemical detection of parts-per-billion lead via an electrode-bound DNAzyme assembly. *J. Am. Chem. Soc.* **129**, 262–263 (2007).
31. Gao, Y. & Li, B. G-quadruplex DNAzyme-based chemiluminescence biosensing strategy for ultrasensitive DNA detection: Combination of exonuclease III-assisted signal amplification and carbon nanotubes-assisted background reducing. *Anal. Chem.* **85**, 11494–11500 (2013).
32. Joos, B., Kuster, H. & Cone, R. Covalent attachment of hybridizable oligonucleotides to glass supports. *Anal. Biochem.* **247**, 96–101 (1997).
33. Chrisey, L. Covalent attachment of synthetic DNA to self-assembled monolayer films. *Nucleic Acids Res.* **24**, 3031–3039 (1996).
34. John, M., Hughes, G. & Andrews, D. W. Preparation of Magnetic Oligo(dT) Particles. **20**, 2–3 (1996).
35. Lamture, J. B. *et al.* Direct detection of nucleic acid hybridization on the surface of a charge coupled device. **22**, 2121–2125 (1994).
36. Piunno, P. A. E., Krull, U. J., Hudson, R. H. E., Damha, M. J. & Cohen, H. Fiber optic biosensor for fluorimetric detection of DNA hybridization. *Anal. Chim. Acta* **288**, 205–214 (1994).
37. Cohen G, Deutsch J, Fineberg J, L. A. Covalent attachment of DNA oligonucleotides to glass. *Nucleic Acids Res* **25**, 911–912 (1997).
38. Varghese, N. *et al.* Binding of DNA nucleobases and nucleosides with graphene. *ChemPhysChem* **10**, 206–210 (2009).
39. Holmberg, A. *et al.* The biotin-streptavidin interaction can be reversibly broken using water at elevated temperatures. *Electrophoresis* **26**, 501–510 (2005).
40. Aguirre, S. D., Ali, M. M., Salena, B. J. & Li, Y. A sensitive DNA enzyme-based fluorescent assay for bacterial detection. *Biomolecules* **3**, 563–577 (2013).
41. Kang, D. K. *et al.* Rapid detection of single bacteria in unprocessed blood using Integrated Comprehensive Droplet Digital Detection. *Nat. Commun.* **5**, 1–10 (2014).
42. Hsieh, P. Y. *et al.* RNA Protection is Effectively Achieved by Pullulan Film Formation.

*ChemBioChem* **18**, 502–505 (2017).

43. Product Data Sheet (Streptavidin Agarose Ultra Performance). Available at: <https://www.trilinkbiotech.com/cart/scripts/prodView.asp?idproduct=14266>.
44. Liu, M. *et al.* A graphene-based biosensing platform based on the release of DNA probes and rolling circle amplification. *ACS Nano* **8**, 5564–5573 (2014).

### 3. Conclusions and future work

#### 3.1. Conclusions

The work documented in this thesis demonstrates that immobilizing RNA-cleaving DNAszymes onto agarose beads is a very effective approach to creating highly sensitive and easy-to-use biosensors that are capable of detecting specific bacteria—in this case, *Escherichia coli* (*E. coli*). In order to identify the optimal immobilization surface, three different materials were tested: reduced graphene oxide, magnetic beads, and agarose beads. Ultimately, agarose beads were selected because they produced the highest signal-to-background ratio. Based on the obtained experimental results, the following conclusions can be made:

- The kinetics of the DNAszyme's activity in solution are essentially the same as when it is immobilized on agarose beads. Thus, immobilizing DNAszyme on agarose beads does not diminish its kinetics of detection.
- Immobilizing the DNAszyme on agarose beads did not diminish its limit of detection (LOD). Both the DNAszyme in solution and the DNAszyme that had been immobilized on agarose beads were able to detect as few as  $10^3$  *E. coli* cells. This is a promising result, as it provides further evidence that this solid-phase assay can be used as the central piece of an *E.coli*-detection biosensor.
- The DNAszyme's specificity remained unaltered after being immobilized on agarose beads, and only the *E.coli* CIM was able to induce cleavage in both the bead-based and solution-based assays.

- A truncation analysis of the DNAzymes in solution and immobilized on agarose beads indicated that the full-length DNAzyme (70 nucleotides) and its truncated sequence (23 nucleotides) had comparable cleavage activity, with slightly faster cleavage activity being observed for the full-length DNAzyme. Both sequences could be useful in biosensor designs; for example, the short-length DNAzyme could be useful when the system needs to be coupled with signal amplification strategies like RCA, and the full-length DNAzyme could be useful when faster cleavage activity is desired.
- The coupling of immobilized DNAzyme on agarose beads and filtration enabled the sensitive detection of *E. coli* in both water samples and complex matrices, such as milk and apple juice. This bead-based assay successfully decreased the non-specific background signal via a simple partitioning step; this is a critical requirement for the development of biosensors with lower limits of detection that is simply not possible using solution-based assays.

Although we have demonstrated the functionality of our *E. coli*-specific DNAzyme bead-based assay, this design can be easily adapted for use with any RNA-cleaving DNAzyme to detect a wide range of bacterial targets.

In summary, this thesis describes the development of a robust, simple, sensitive, and cost-effective bead-based assay for the detection of bacteria using DNAzymes. Given its ability to eliminate the need for specialized equipment and trained personnel, this assay is a highly attractive option for field applications, especially in resource-limited regions. Thus, this work is a

stepping-stone in the development of practical biosensors that can eventually be used to monitor our health, safeguard our food and water, and protect our environment.

### **3.2. Future work**

The results and findings in this work indicate that bead-based biosensors possess considerable potential for future development. Therefore, the following avenues for future research are recommended based on the results of this research:

- The development of a colorimetric assay using gold nanoparticle-tagged DNAzyme that allows the signal to be detected by the naked eye.
- The development of multiplex biosensing via the incorporation of multiple DNAzyme for different bacteria. This would enable multiplex high-throughput bacteria detection in food and water.
- The development of new bacteria-specific DNAzyme probes through *in vitro* selection and implementing them in the developed platform to target desired bacteria in food and water.
- The development of a single-step “Beads to Paper” assay for signal concentration and improving the detection sensitivity.